FORSCHUNGSZENTRUM JÜLICH GmbH

KFA

Institut für Plasmaphysik
Association EURATOM-KFA

The Rôle of Molecular Hydrogen in Plasma Recombination

P. T. Greenland D. Reiter

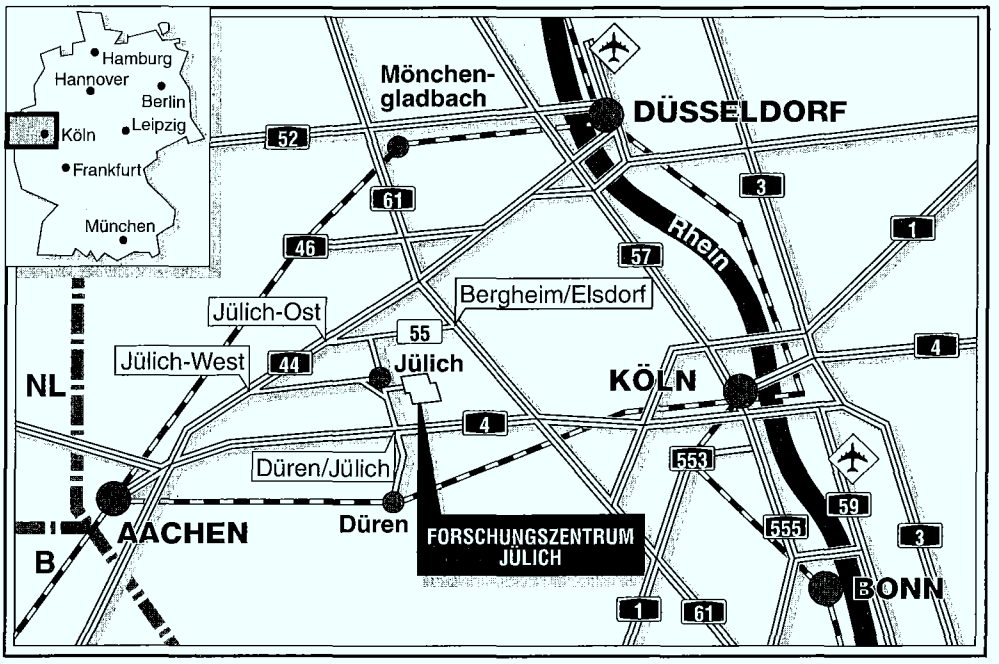

Berichte des Forschungszentrums Jülich ; 3258
ISSN 0944-2952
Institut für Plasmaphysik Jül-3258
Association EURATOM-KFA

Zu beziehen durch: Forschungszentrum Jülich GmbH · Zentralbibliothek
D-52425 Jülich · Bundesrepublik Deutschland
Telefon: 02461/61-6102 · Telefax: 02461/61-6103 · Telex: 833556-70 kfa d

The Rôle of Molecular Hydrogen in Plasma Recombination

P.T. Greenland[1] D. Reiter[2]

[1] Work performed under KFA-contract 41-295-383
Optics Section, Blackett Laboratory, Imperial College, London SW7 2BZ, UK
[2] Forschungszentrum Jülich GmbH, D-52425 Jülich, FRG

Abstract

We consider the effect of the presence of molecular hydrogen on plasma recombination at temperatures of a few electron volts. The rôle of 2-body processes such as ion conversion and dissociative attachment in accelerating the recombination is exposed, both in a simplified model, which can be solved analytically, and in more realistic numerical calculations. All the important atomic and molecular processes are included in a set of non-linear rate equations, from which we identify the important parameters of the model and thereby show which cross sections are critical.

Although we do not include transport explicitly we are able to extend the model to mimic recycling at the plasma edge. This enables us to demonstrate the importance of the contribution of H_2 to recombination. Our model is primitive, but it enables us to identify processes which are important in modelling H_2-plasma interactions, and which will therefore have to be treated in more complex plasma codes. We find that some of the ideas basic to atomic modelling of plasmas may have to be revised if molecular processes are important in the plasma dynamics. In particular, the non-linearities we discuss lead to instabilities, which allow the co-existence of several solutions for the same physical parameters.

1. Introduction

At low temperatures, below a few eV, bulk plasma recombination is slow, because radiative recombination is inefficient, and three body combination requires high densities to be effective. However, molecular hydrogen can exist in the plasma and it has long been thought (Janev, *et al* 1984, Krasheninnikov, Pigarov and Sigmar 1996) that the presence of molecules could be important in accelerating recombination at low temperature, because the two-body processes of dissociative attachment (DA)

$$e + H_2 \rightarrow H + H^- \tag{1}$$

and ion conversion (IC)

$$p + H_2 \rightarrow H + H_2^+ \tag{2}$$

followed by mutual neutralization (MN)

$$p + H^- \rightarrow H + H \tag{3}$$

and dissociative recombination (DR)

$$e + H_2^+ \rightarrow H + H \tag{4}$$

effectively lead to the recombination of plasma electrons and protons, through a series of fast 2-body interactions. (This is not a catalytic process, because the H_2 is consumed.) However, because of the strong dependence of the rates for these processes on the vibrational state of the molecule, and the large number of new atomic and molecular processes which can occur when molecules are involved, only crude estimates of the importance of molecules in accelerating recombination have been made. Since we have reasonable estimates for all the rates that contribute (Janev *et al* 1987, see appendix 1), we can set up equations for, and solve, the intrinsically non-linear recombination problem. The presence of molecules introduces new physical phenomena, some of which violate the usual assumptions made in modelling fusion plasmas. In this work our main concern is to expose what can happen when molecular hydrogen interacts with the edge plasma, first because it is indeed a constituent of the low temperature edge region of fusion plasmas, and secondly in order to identify the important atomic and molecular processes which contribute to the neutralization. This will enable us to identify which cross sections are critical, and thus to specify future data needs more accurately.

In order to simplify the problem as much as possible, we do not consider transport, that is, we confine our attention to a zero dimensional model. However, an important feature of this study is that we take particular care

to model all the processes explicitly. We treat all the molecular vibrational levels, and make no assumptions about plasma neutrality or the relative magnitude of the densities of specific species. Nor do we assume stationary plasma conditions. As a result, we are faced with a set of non-linear rate equations to solve.

Of course, a problem of this complexity requires a numerical solution, and we give details in section 3. In sections 4 and 5 we adapt the results to a more realistic situation, but in order to understand these results fully we require some guidance. This we obtain from a truncated, but still non-linear model which isolates the important physics of the molecule assisted recombination process, and, surprisingly, can be solved analytically. We discuss this in section 2. Section 6 is a summary.

2 An analytic model

We shall find that of the two processes mentioned above, ion conversion followed by dissociative recombination is often the more important. Therefore we consider a model which contains H_2, p, e, H_2^+ and H. The rate equations we solve are:

$$\dot{n}_{H_2} = -S_p n_{H_2} n_p + \Gamma \tag{5a}$$

$$\dot{n}_p = -S_p n_{H_2} n_p \tag{5b}$$

$$\dot{n}_{H_2^+} = S_p n_{H_2} n_p - S_{DR} n_{H_2^+} n_e \tag{5c}$$

$$\dot{n}_e = -S_{DR} n_{H_2^+} n_e \tag{5d}$$

We shall not consider the H explicitly, but its equation of motion is

$$\dot{n}_H = 2S_{DR} n_{H_2^+} n_e + S_p n_{H_2} n_p - \Gamma_H \tag{5d}$$

where we have assumed that the flow of molecular hydrogen into the plasma with effective source Γ is balanced by a flow of atomic hydrogen out of the plasma with sink Γ_H. This is depicted in figure 1.

Below, we show how the effective ion conversion rate S_p and molecule source[1] Γ can be related to the physical rates S_k^{IC} and source Γ_{mol} when other molecule-destroying processes compete with ion conversion. First, we consider the solution of 5.

We have the following strict conservation laws:

[1]Quantities like Γ are source terms with dimension $L^{-3}T^{-1}$, and we refer to them as such in this report. In a model which properly included transport, they would be related to particle fluxes (with dimension $L^{-2}T^{-1}$), and we often speak of them *as if* they were fluxes.

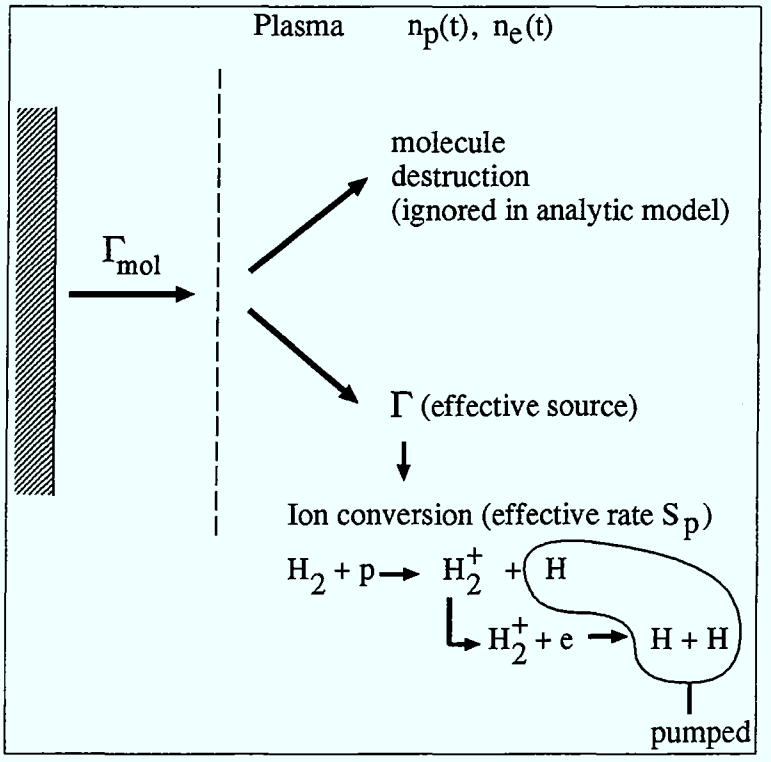

Figure 1. The physical problem described by the analytic model

1. Particle balance

$$\dot{n}_{H_2} + \dot{n}_p + \dot{n}_{H_2^+} + \dot{n}_e + \dot{n}_H = \Gamma - \Gamma_H \tag{6a}$$

2. Proton balance

$$2\dot{n}_{H_2} + \dot{n}_p + 2\dot{n}_{H_2^+} + \dot{n}_H = 2\Gamma - \Gamma_H \tag{6b}$$

3. Electron balance

$$2\dot{n}_{H_2} + 2\dot{n}_{H_2^+} + \dot{n}_e + \dot{n}_H = 2\Gamma - \Gamma_H \tag{6c}$$

4. Charge conservation

$$\dot{n}_p + \dot{n}_{H_2^+} - \dot{n}_e = 0 \tag{6d}$$

We begin by solving for n_p, on the assumption that at t=0 the proton and electron densities are both n_0, and there is no H_2. Subtracting (5a) from (5b) and integrating gives

$$n_p(t) - n_{H_2}(t) = n_0 - \Gamma t \tag{7}$$

which, with (5b) gives an equation for the proton density

$$\dot{n}_p = S_p n_p (n_0 - \Gamma t - n_p) \tag{8}$$

This equation is of the form

$$\dot{y} = y(Z'(t) - Ay) \tag{9}$$

and it is straightforward to verify that its solution is given by

$$y(t) = \frac{y_0 F'(t)}{1 + y_0 A F(t)} \tag{10}$$

where

$$F(t) = \int_0^t \exp[Z(t')]\, dt' \tag{11a}$$

and

$$Z(t) = \int_0^t Z'(t')\, dt' \tag{11b}$$

and, of course $y_0 = y(0)$.

Applying this to equation (8) gives

$$n_p(t) = \frac{n_0 \exp[-(\alpha - \beta t)^2]}{e^{-\alpha^2} + \sqrt{\pi}\alpha\{\mathrm{erfc}[\alpha - \beta t] - \mathrm{erfc}[\alpha]\}} \tag{12}$$

with

$$\alpha = n_0 \left(\frac{S_p}{2\Gamma}\right)^{\frac{1}{2}} \tag{13a}$$

$$\beta = \left(\frac{S_p \Gamma}{2}\right)^{\frac{1}{2}} \tag{13b}$$

and

$$\mathrm{erfc}(z) = \frac{2}{\sqrt{\pi}} \int_z^\infty e^{-t^2}\, dt$$

(Abramowitz and Stegun 1970)

In order to proceed we must make some assumptions about the molecular hydrogen. The equation of motion for v_k, the density of its k'th vibrational state is

$$\dot{v}_k = n_e \left[\mathbf{M}_0 \cdot \mathbf{v}\right]_k - \{S_k^{DA} n_e + S_k^{Diss} n_e + S_k^{IC} n_p\} v_k + \Gamma_{mol} \gamma_k \tag{14}$$

where $\mathbf{M}_0$ is the $(N_v \times N_v)$ rate matrix for the purely vibrational couplings amongst the N_v vibrational levels[2], and S_k^{DA}, S_k^{Diss} and S_k^{IC} represent dissociative attachment, direct electron impact dissociation and ion conversion from level k respectively. The H_2 source Γ_{mol} has been resolved into its vibrational components using the vector γ, where γ_k is, of course, the relative occupancy of the vibrational state k in the incoming source. The total H_2 density is

$$n_{H_2} = \sum_{k=1}^{N_v} v_k \tag{15}$$

Since we assume $\sum \gamma_k = 1$, the total H_2 source is just Γ_{mol}.

We make the assumption that the H_2 rapidly comes to vibrational equilibrium with its environment, and solve equation 14 for the equilibrium populations v_k^{eq}

$$v_k^{eq} = -\frac{\Gamma_{mol}}{n_0} \left[(\mathbf{M}_0 - \mathbf{S})^{-1} \gamma\right]_k \tag{16}$$

where $\mathbf{S}$ is a diagonal matrix whose (k,k)'th element is the total rate coefficient for loss of molecules from level k. We have assumed that only electron and proton collisions can lead to loss of H_2 and that $n_e = n_p = n_0$. It is convenient to define the two quantities

$$f = -\sum_{k=1}^{N_v} \left[(\mathbf{M}_0 - \mathbf{S})^{-1} \gamma\right]_k / n_0 \tag{17}$$

[2]We assume that only electron collisions are responsible for vibrational excitation

which represents the survival time for a molecule and r_0, the ratio of the H_2 equilibrium density to the initial plasma electron (or proton) density, so that

$$r_0 = \frac{n_{H_2}^{eq}}{n_0} = \frac{\sum_{k=1}^{N_v} v_k^{eq}}{n_0} \tag{18}$$

We have

$$r_0 = \frac{f\,\Gamma_{mol}}{n_0} \tag{19}$$

We must now relate S_p and Γ, the parameters of the model equations (5) to the physical processes represented by the rates S_k^{DA}, S_k^{Diss} and S_k^{IC}, and the source of molecules Γ_{mol}. In our simple model the only H_2 loss mechanism is ion conversion at a rate given by $S_k^{IC} n_p$ from the k'th vibrational level. This is also the effective rate coefficient for the production of H_2^+. However, in general the H_2 destruction rate is larger than the H_2^+ production rate. We accommodate this in the simple model by adjusting S_p and Γ. We obtain S_p the H_2^+ production rate in equations (5b) by averaging S_k^{IC} over the vibrational level density, so that we have, initially

$$S_p = \frac{\sum_{k=1}^{N_v} v_k^{eq} S_k^{IC}}{\sum_{k=1}^{N_v} v_k^{eq}} \tag{20}$$

and we assume this is true for all time. The effective H_2 source Γ is related to the true molecular source Γ_{mol} by considering the equilibrium H_2 concentration. In the simple model, this is given by equation (5a) as

$$\frac{\Gamma}{S_p n_0}$$

Equating this with $\sum v_k^{eq}$ from equation (16) gives

$$\Gamma = n_0 S_p f \Gamma_{mol} = -\left\{ \sum_{k=1}^{N_v} S_k^{IC} \left[(\mathbf{M}_0 - \mathbf{S})^{-1} \gamma \right]_k \right\} \Gamma_{mol} \tag{21}$$

In general $\Gamma < \Gamma_{mol}$. However, if ion conversion is the only mechanism for the destruction of H_2, equation (21) can be simplified. The sum $\sum_k M_{0\,(k,j)} = 0$ for all j, and, in the case that ion conversion is the only H_2 destruction mechanism $\mathbf{S}_{k,k} = S_k^{IC}$. Under this circumstance it is straightforward to show that the sum $\{\cdots\}$ in equation (21) is equal to -1, so that, in this case we have

$$S_p = \frac{1}{f n_0} = \frac{\Gamma}{r_0 n_0^2} \tag{22}$$

and $\Gamma = \Gamma_{mol}$. Physically equation (21) implies that Γ, the source to be used in the model equations corresponds to a source of molecules which are 'effective', in producing H_2^+. Molecules which are destroyed, but do not produce H_2^+ must not be counted as effective neutralizers. Only if each H_2 destruction produces an H_2^+ do we have $\Gamma = \Gamma_{mol}$. Finally it is important to notice that both S_p and Γ can be calculated from the dynamics of the H_2 vibrational excitation by a simple matrix inversion.

We now consider the proton density, equation (12). Equations (13a), (19) and (21) imply that

$$\alpha = \left(\frac{1}{2r_0}\right)^{\frac{1}{2}}$$

and since we are dealing with small equilibrium H_2 concentrations, α is a large number. We may therefore always use the asymptotic expansion for erfc[α], and provided $|\alpha - \beta t| \gg 1$ we can also expand erfc[$\alpha - \beta t$]. This gives the following results:

1. $t \ll t_0 = \alpha/\beta = n_0/\Gamma$

$$n_p(t) \sim n_0 - \Gamma t + \frac{\Gamma}{S_p(n_0 - \Gamma t)} \tag{23a}$$

2. $t = t_0$

$$n_p(t_0) \sim \frac{n_0}{\sqrt{\pi}\alpha} \tag{23b}$$

3. $t \gg t_0$

$$n_p(t) \sim \frac{n_0 \exp[-(\alpha - \beta t)^2]}{2\sqrt{\pi}\alpha} \tag{23c}$$

Finally, it is straightforward to show that for times $t \ll t_0$ (but still $t \gg f$) the concentration $r(t)$ behaves as a function of time as

$$r(t) = r_0(1 + \frac{2t}{t_0})$$

Thus, we can identify three temporal ranges: an initial, more or less linear fall in proton density at a rate given by Γ, a transitional region near $t \sim t_0$, and a rapid fall—faster than exponential—for large times. In appendix 2 we give details of how these results for the proton density can be used to get the H_2, electron and H_2^+ densities[3]. Simple results can only be obtained in the asymptotic regions:

[3]The H_2 density can be derived easily using equation (7). In the initial region we have, approximately, $n_{H_2} \sim \Gamma/[S_p(n_0 - \Gamma t)]$

For $t \ll t_0$:

$$n_e(t) \sim n_0 - \Gamma t + \frac{(S_p + S_{DR})\Gamma}{S_p S_{DR}(n_0 - \Gamma t)} \tag{24}$$

$$n_{H_2^+}(t) \sim \frac{\Gamma}{S_{DR}(n_0 - \Gamma t)} \tag{25}$$

and for $t \gg t_0$:

$$n_e(t) \sim n_{H_2^+} \sim \frac{n_1}{1 + S_{DR} n_1 (t - t_1)} \tag{26}$$

The effective density n_1 and time t_1 are discussed in appendix 2. Notice that the characteristic time for changes in density $t_0 = n_0/\Gamma$ can be related to the vibrational equilibration time f through

$$t_0 = \frac{\Gamma_{mol}}{r\Gamma} f \gg f \tag{27}$$

so that the assumption that vibrational equilibration is much faster than changes in density is indeed valid.

Thus, we see that the effect of H_2 on plasma neutralization can be characterized as follows. As H_2 flows into the plasma it comes to vibrational equilibrium, on a time-scale given by f, and the plasma protons are neutralized by ion conversion. The resulting H_2^+ is neutralized by the plasma electrons by dissociative recombination. This is usually a much faster process than ion conversion so that the H_2^+ density is kept small and follows the H_2 density. In this period the neutralization rate is determined by the availability of H_2. As the proton and electron densities fall, the concentration of H_2 grows—there are fewer protons and electrons to destroy the molecular hydrogen—so that the protons are more rapidly neutralized and their density falls dramatically. Now all the positive charge is carried by the H_2^+, which recombines with the electrons with a $1/t$ law, just as in radiative recombination, but at a much faster rate determined by S_{DR}. We now give some numerical examples.

3. The numerical solutions

First, we compare the analytic and numerical solutions of equation 5. The numerical solutions are obtained by using Gear's method, and serve to test the two assumptions made deriving the analytic solutions—first, that vibrational equilibrium is rapidly established, and secondly that the initial vibrational distribution can be used for all time. We present results for the following set of standard parameters:

Plasma temperature	3 eV
Initial H_2 vibrational state	$v = 0$
Initial e & p densities n_0	10^{13} cm^{-3}
Equilibrium H_2 concentration r_0	0.01
H_2 source Γ_{mol}	$n_0 r_0/f$ (eqn. 19)

Table 1.

Figure 2 compares the exact analytic expression (12), and the numerical result for the proton density. It can be seen that the agreement is good for $t < t_0$, but that there are deviations in the analytic and numerical results for large times. This can be attributed to the assumption that vibrational equilibrium is maintained as the charged particle densities drop. That this is not the case is shown in figure 3. We see that as the proton and electron densities drop, the distribution of H_2 vibrational levels changes. Thus the effective parameters S_p, Γ, f *etc* also change. This is properly included in the numerical, but not the analytic result. However, the important features of the full numerical solution are indeed given by the analytic result, in particular the characteristic time t_0 can be obtained from equation 12, and for times less than this the H_2^+ density follows the the H_2 density, but reduced by a factor of S_p/S_{DR}. Finally figures 4 and 5 show the very early time behaviour of the charged particle and H_2 vibrational level densities. We do indeed find that vibrational equilibrium is established on a timescale given by f.

Finally, in figure 6, we show the effect of including dissociative attachment (DA). It is clear that ion conversion is indeed the dominant process, at least for the conditions considered here.

Equations (17), (20) and (27) can be used to calculate the effective equilibration and decay times f and t_0, as well as the sources Γ_{mol} required to get an initial equilibrium concentration of $r_0 = 0.01$. The results of such a calculation are shown in table 2.

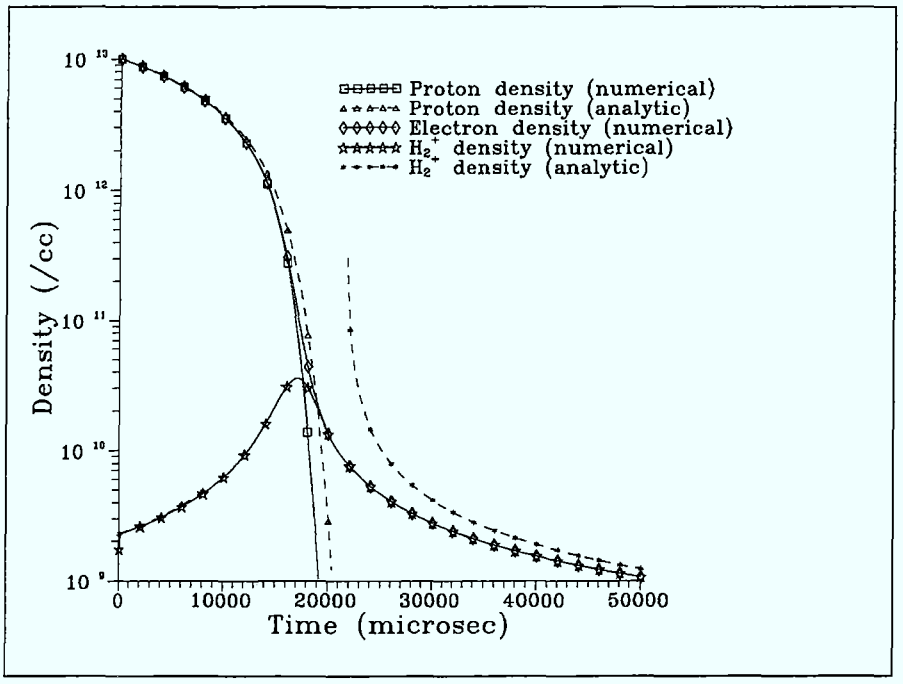

Figure 2. Comparison of analytic and numerical results when ion conversion and direct electron impact dissociation are included

	no H^-	with H^-
f (μs)	60.35	59.39
t_0 ms	15.12	15.66
S_p (cm^3/s)	6.5×10^{-10}	6.4×10^{-10}
Γ_{mol} cm^{-3}/s	1.66×10^{15}	1.68×10^{15}
$r(t_0/10)$ (numerical results)	0.0121	0.0122

Table 2.

and it is clear from the figures that these values are in agreement with the numerical calculations.

In the foregoing discussion, we have neglected two important processes; H_3^+ production and electron impact ionization of atomic hydrogen. For the sake of completeness we show, in figures 7 and 8, the result of including H_3^+ production. Although the effect on the distribution of H_2 vibrational states is small, there is a considerable effect on the distribution of charged particles. We see that H_3^+, rather than H_2^+ becomes the principal positive charge carrier

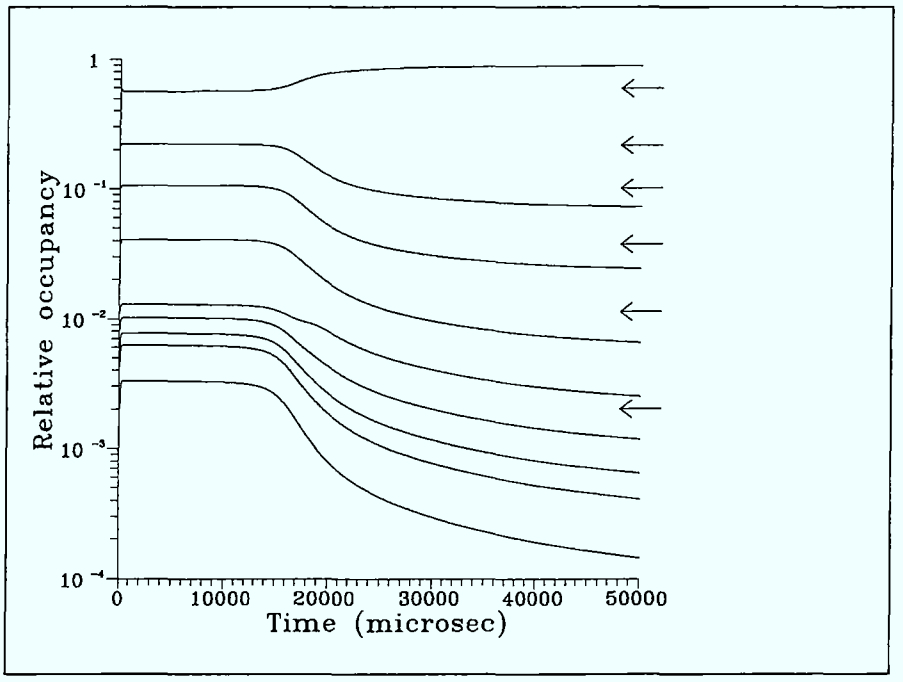

Figure 3. The distribution of vibrational states in H_2. The relative occupancy of the first 8 states and the last state (15) are shown as a function of time. The arrows mark the equilibrium values for levels 1 to 5 and 15 according to equation 16

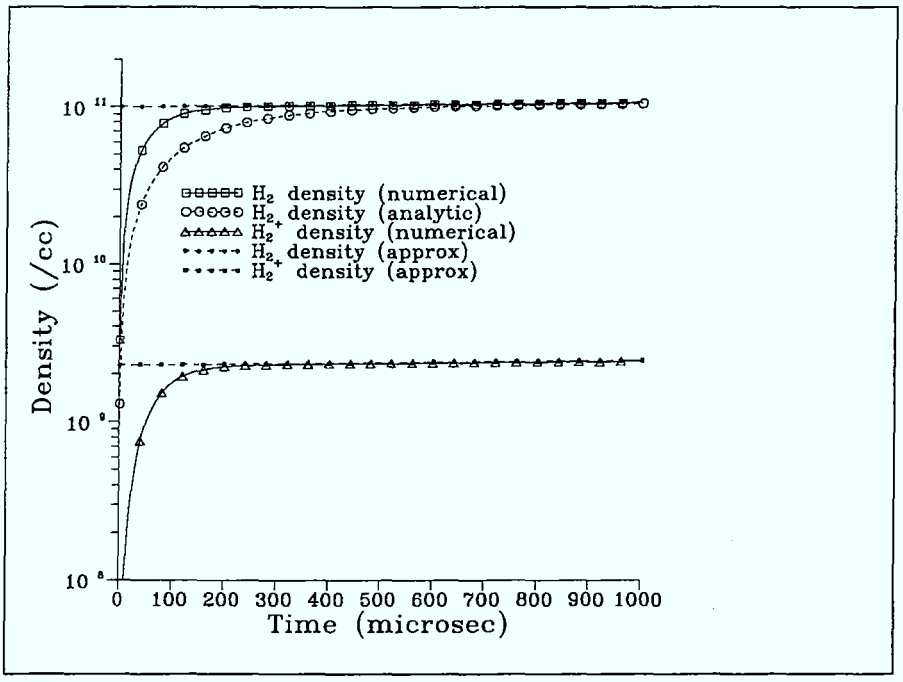

Figure 4. As for figure 2 but for small times

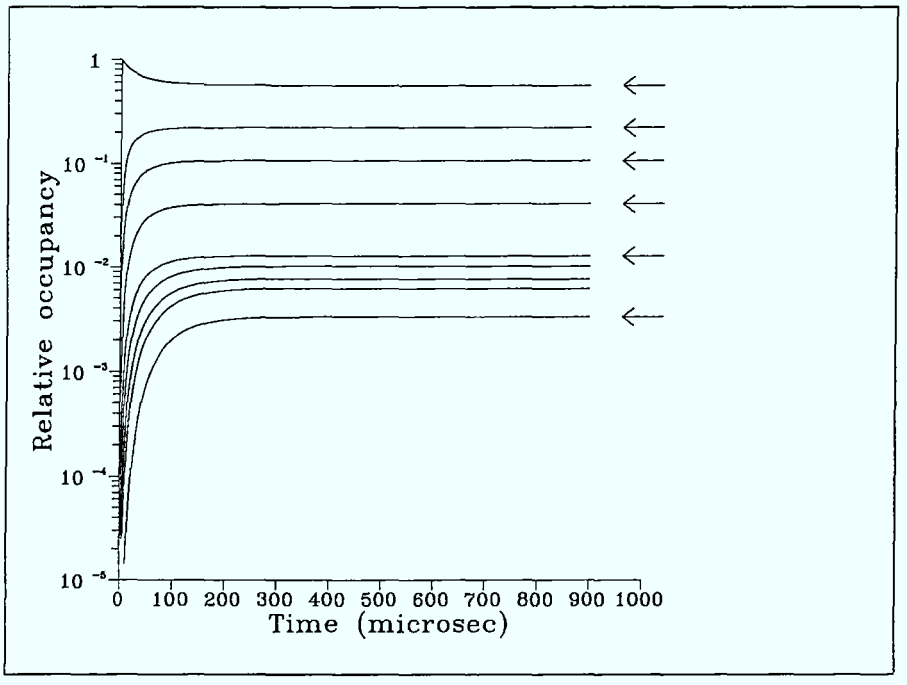

Figure 5. As for figure 3 but for small times

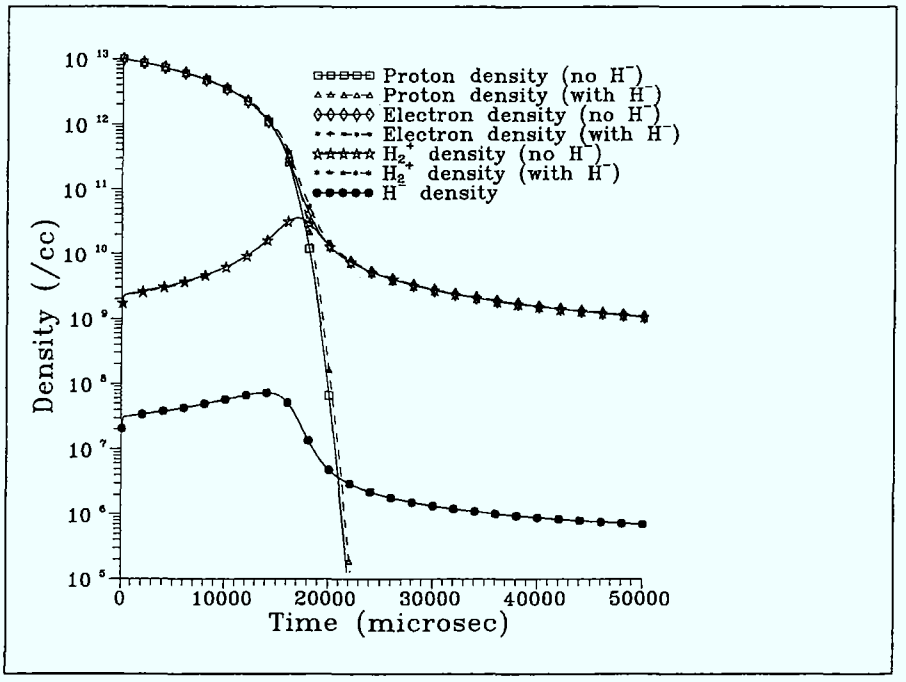

Figure 6. Comparison between the numerical results both with and without dissociative attachment channels

after the proton density collapses. This is because the H_2^+ density also suffers a collapse, in complete analogy to the proton density collapse as the processes

$$H_2 + H_2^+ \rightarrow H + H_3^+$$

and

$$e + H_3^+ \rightarrow H + H_2$$

replace ion conversion and dissociative recombination (equations 2 and 4) as the main neutralization mechanism. We consider electron impact ionization of the neutral hydrogen in the next section, and conclude by summarizing the results of the analytic model.

The analytic model has three important parameters; f (equation (17)), the timescale for the establishment of vibrational equilibrium in H_2, t_0 (equation (23a)), the timescale on which particle concentrations vary before proton collapse, and Γ, (equation (21)), the effective H_2 source. In the model, a source of H_2 leads to neutralization, mainly through IC, so that the H_2 density grows relative to the proton density, which ultimately collapses, leaving H_2^+ as the main positively charged species[4]. A more realistic picture must include

[4]Or H_3^+ if its production is included.

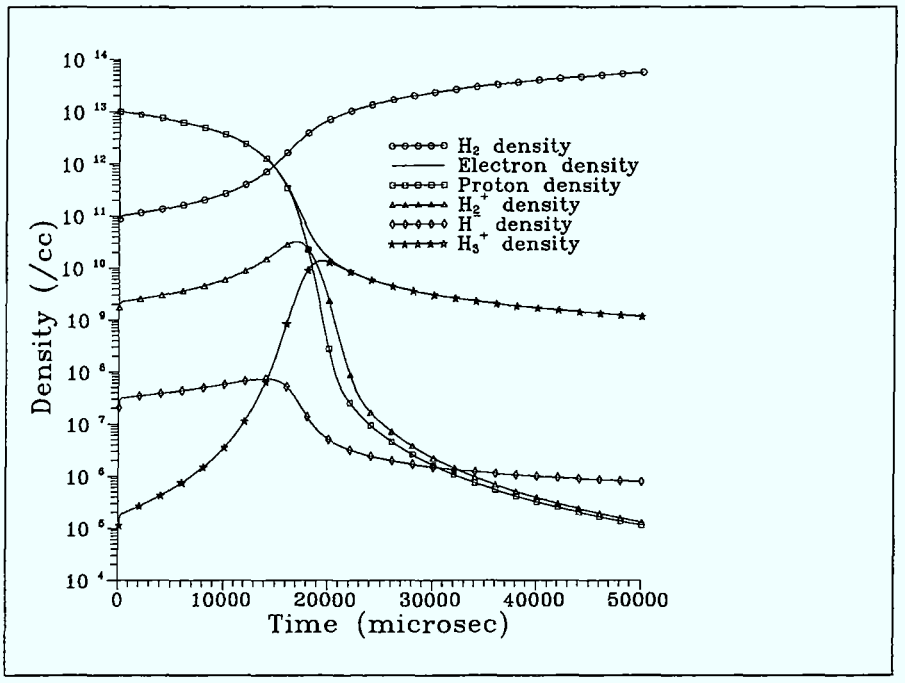

Figure 7. The effect of including H_3^+ production on the particle densities (*cf* figure 6)

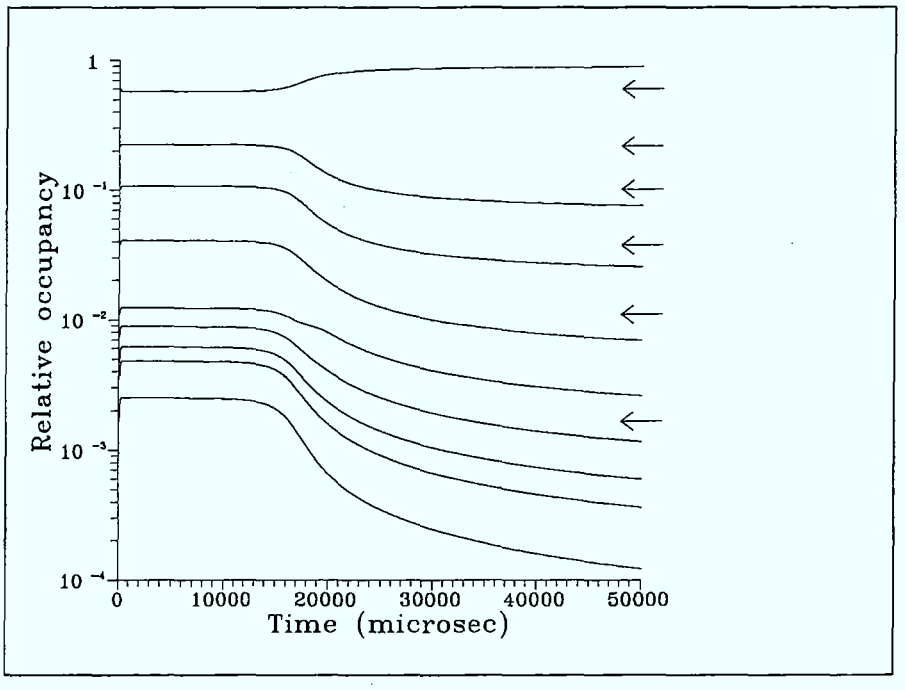

Figure 8. As for figure 3 but including H_3^+ production

two features which our analytic model lacks. First, in contrast to what we have assumed, the electron impact ionization of the atomic H produced in these processes is not negligible at eV temperatures, and secondly, particle transport is important near the plasma edge. We consider both of these phenomena in the next section.

4. Recycling.

The analytic model described in the previous sections does indeed confirm that H_2 plays an important rôle in plasma neutralization, and illuminates the complex behaviour which occurs when several molecular species are involved in the neutralization process. However, in order to make contact with the real physics of H_2 in the plasma edge we must extend the model in two ways. First, the main product of the processes described above is atomic hydrogen, and its fate must be considered in greater detail. The simple model we have been discussing does not include electron impact ionization of atomic H, so there is no channel to replenish the protons consumed by ion conversion. Were such a channel to exist, the behavior of the proton density would ultimately rise without limit, as incoming H_2 converts to protons. This is clearly temperature dependent. If the electron temperature is high enough for impact ionization of H (and dissociative ionization of H_2, H_2^+ *etc*) to be significant, then the proton density will not collapse, but will rise as the incoming H_2 is converted, ultimately, to protons. On the other hand, if the temperature is low enough that the proton destruction rate through IC dominates initially we may expect a collapse, followed by a slow rise in proton density as ionization takes over. We return to this point in section 6.

Secondly, the picture of a plasma with a given density of electrons and protons contaminated by an external source of H_2 is too limiting. and we shall extend it. The important physical processes are shown in figure 9.

First, we assume that the edge plasma is produced by a source of protons Γ_p and an equal source of electrons from the plasma interior, balanced by loss mechanisms, which we model by introducing three characteristic times τ_p, τ_H and τ_{mol}; τ_p is the confinement time for protons, and τ_H the confinement time for neutral hydrogen. We assume that all the heavy charged particles have confinement times related to τ_p through

$$\tau_S = \sqrt{\frac{M_S}{M_p}}|\frac{q_S}{q_p}|\tau_p \tag{28}$$

where τ_S is the confinement time for species S, which has mass M_S and charge q_S. The electron confinement time adjusts itself to maintain plasma

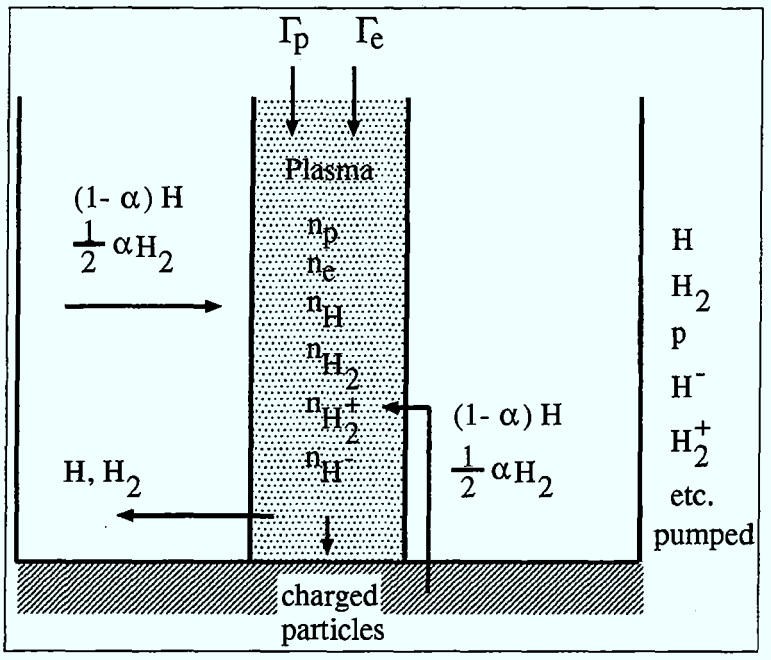

Figure 9. The physical problem described by the recycling model

neutrality. Thus, in the absence of any other mechanisms, the plasma density comes to equilibrium with

$$n_p = n_e = \Gamma_p \tau_p \tag{29}$$

However, we assume that some fraction of the particles escaping from the plasma are recycled, and re-enter the plasma, either as H or H_2. This H_2 has a confinement time of τ_{mol}. Because the molecules are heavier than the atoms, and, in general are not in thermal translational equilibrium with the plasma, we usually have $\tau_{mol} > \tau_H$.

Since charged particles are only free to move along the magnetic field, the proton confinement time τ_p is given by the connection length divided by the proton velocity, *i.e.*

$$\tau_p \sim \frac{\pi q R}{\sqrt{\frac{2kT}{m_p}}} \sim 3 \text{ ms} \tag{30a}$$

where q is the safety factor and R the major radius, and we assume that the parallel drift velocity is comparable to the proton thermal velocity at plasma temperature T. The numerical result corresponds to a temperature of 3 eV and a connection length of $\sim$ 72 m, a value typical of the ITER design. We take 3 ms as typical for the proton confinement time in all our calculations. The corresponding confinement time for neutral hydrogen,

which is not constrained to follow the magnetic field lines is correspondingly shorter, and we have

$$\tau_H \sim \frac{L_x}{\sqrt{\frac{2kT}{m_p}}} \sim 1.3 \ \ \mu\text{s} \tag{30b}$$

where L_x is a characteristic distance for cross field transport, which we take to be 3 cm. Once again the numerical result is for a temperature of 3 eV.

Now suppose that the particles which leave the plasma are recycled. We start by assuming that there is no H_2, so that the plasma consist of e, p and H. We assume that a fraction d_c of the charged particles and a fraction d_H of the hydrogen are pumped, but the rest re-enter the plasma as H. Thus, the rate equations are

$$\dot{n}_p = \Gamma_p + S(n_e,T)n_0 n_e - \alpha(n_e,T)n_p n_e - n_p/\tau_p \tag{31a}$$

$$\dot{n}_e = \Gamma_e + S(n_e,T)n_0 n_e - \alpha(n_e,T)n_p n_e - n_e/\tau_e \tag{31b}$$

$$\dot{n}_0 = \frac{1-d_H^{\text{eff}}}{\tau_H}(n_0 + n_{ex}) + \frac{1-d_c^{\text{eff}}}{\tau_p}n_p + \alpha(n_e,T)n_e n_p - S(n_e,T)n_0 n_e - n_0/\tau_H \tag{31c}$$

where n_p is the proton density, n_e the electron density, n_0 the *ground state* H density and n_{ex} the total excited state hydrogen density. $S(n_e,T)$ and $\alpha(n_e,T)$ are the effective collisional ionization and recombination coefficients respectively. They are supposed to have been derived from an appropriate collisional-radiative (CR) model, (which also gives n_{ex}), and are (electron) density and temperature dependent. Our CR model differs slightly from what is usual in that we include loss mechanisms in the effective rates. If this is not done, then particle number is not conserved, because excited state H is recycled into the ground state. We discuss the details of this model in appendix 3, where the effective destruction fractions d_c^{eff} and d_H^{eff} are defined.

For plasma neutrality we must have $\Gamma_p = \Gamma_e$ and $\tau_p = \tau_e$, so that equations (31a) and (31b) imply that $n_e = n_p$. At equilibrium we must have $\dot{n}_e = \dot{n}_p = \dot{n}_0 = 0$, whence we obtain

$$\Gamma_p + S(n_p,T)n_0 n_p - \alpha(n_p,T)n_p^2 - n_p/\tau_p = 0 \tag{32a}$$

and

$$\Gamma_p - \frac{d_H^{\text{eff}}}{\tau_H}n_0 - \frac{d_p^{\text{eff}}}{\tau_p}n_p = 0 \tag{32b}$$

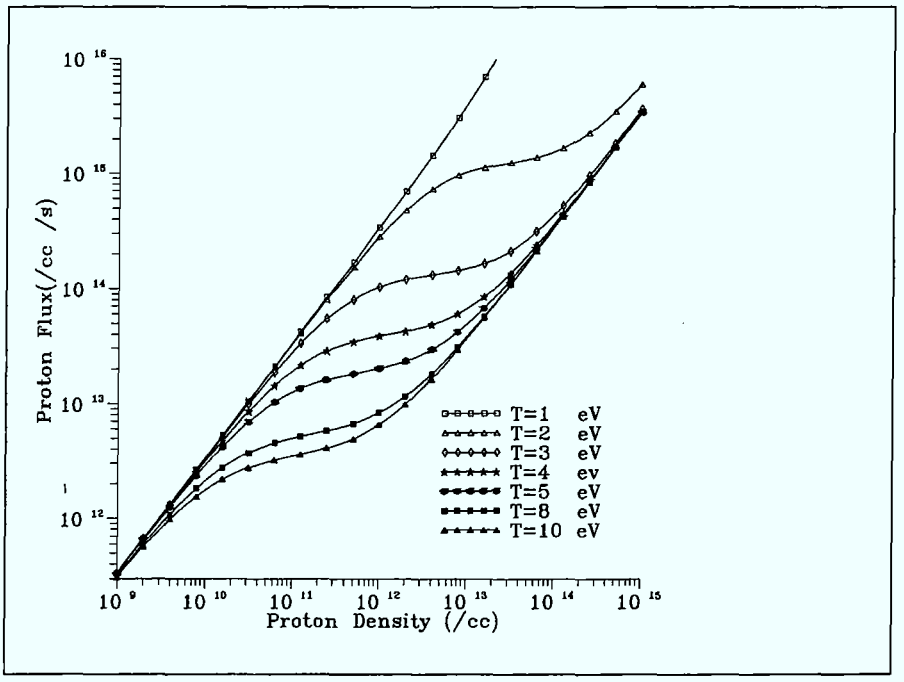

Figure 10. The proton source required to produce a given equilibrium proton density for various temperatures. The confinement times are τ_p=3 ms and τ_H=1.3 μs for all temperatures. The destroyed fractions are $d_c = 0.01$ and $d_H = 10^{-4}$. There is a one-to-one correspondence between Γ and n_p, and all equilibria are stable.

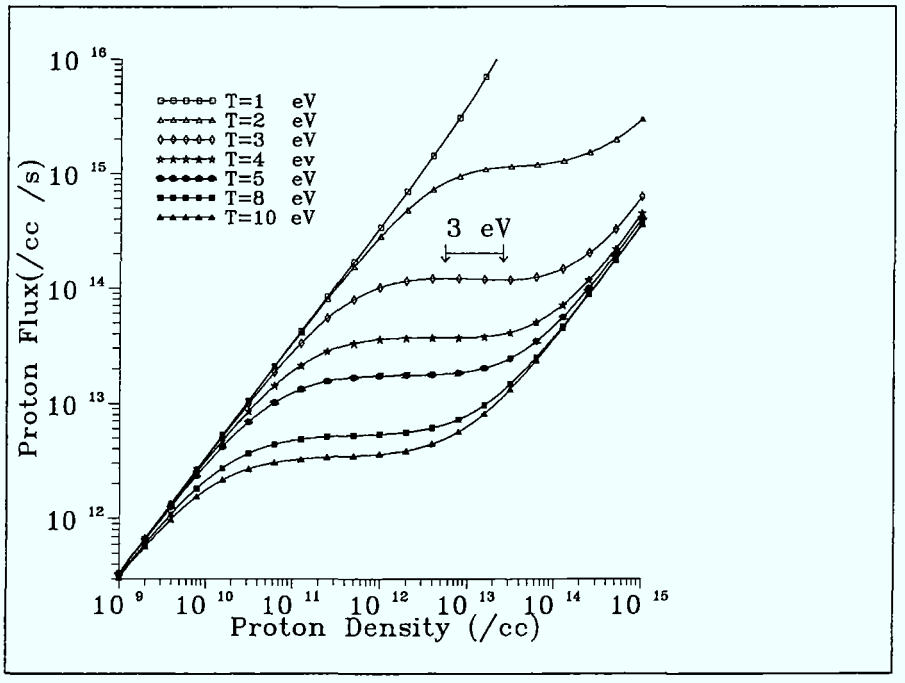

Figure 11. As for figure 10, but for $d_c = 0.001$. Now, for some temperatures, certain values of Γ correspond to three values of n_p, and not all equilibria are stable. The regions of instability are marked.

We may use these equations to determine the equilibrium. If S and α were density *independent* the situation would be simple. Equations 32 would reduce to a quadratic in n_p with the property that a positive solution could be found for any value of the other parameters—τ_p, Γ_p *etc*—and, furthermore, the equilibrium would always be stable. This is not the case if S and α are density dependent. It is easy to show that, for a given n_p we have

$$\Gamma_p = \frac{1}{d_H^{\text{eff}}/\tau_H + Sn_p}\left[(S\frac{d_c^{\text{eff}}}{\tau_p} + \alpha\frac{d_H^{\text{eff}}}{\tau_H})n_p^2 + \frac{n_p}{\tau_p}\frac{d_H^{\text{eff}}}{\tau_H}\right] \tag{33a}$$

and

$$n_0 = \frac{\alpha n_p^2 + (1 - d_c^{\text{eff}})n_p/\tau_p}{Sn_p + d_H^{\text{eff}}/\tau_H} \tag{33b}$$

where, of course S and α are evaluated at n_p. However, the Jacobian matrix at equilibrium $\mathbf{J}$ can be shown to be

$$\mathbf{J} = \begin{bmatrix} q - L & Sn_p \\ L - q - \frac{d_c^{\text{eff}}}{\tau_p} - \gamma & -Sn_p - \frac{d_H^{\text{eff}}}{\tau_H} \end{bmatrix} \tag{34}$$

where

$$\begin{aligned} L &= \frac{\Gamma}{n_p} + \alpha n_p \\ q &= n_0 n_p \frac{\partial S}{\partial n_p} - n_p^2 \frac{\partial \alpha}{\partial n_p} \\ \gamma &= \frac{d_H}{\tau_H}\left[\frac{\partial \bar{v}}{\partial n_p} n_0 + \frac{\partial \bar{r}}{\partial n_p} n_p\right] \end{aligned}$$

($\bar{v}$ and $\bar{r}$ are defined in appendix 3.) The Jacobian matrix shows how the solution to equations 31 behaves near the equilibrium defined by equations 32. If the vector $\delta\mathbf{n} = \{\delta n_p, \delta n_0\}^T$ represents the deviation from equilibrium, then the equation of motion for $\delta\mathbf{n}$ is

$$\dot{\delta\mathbf{n}} = \mathbf{J}\delta\mathbf{n} \tag{35}$$

so that the eigenvalues of $\mathbf{J}$ determine the stability of the solution. In general we find γ in equation 34 is positive. Then it is straightforward to show that unless q is strictly greater than zero[5], both eigenvalues of $\mathbf{J}$ must have negative real part, so the equilibrium is stable. In short, for positive γ, $q > 0$ is a necessary (but not sufficient) condition for unstable or cyclic motion.

[5]Or γ becomes negative

Figures 10 and 11 show the relationship between proton source and proton density for a series of temperatures, and various fixed values of confinement times and destroyed fractions. In figure 10 we show the relationship when 1% of the outgoing protons (and 0.01% of the H) are destroyed. For these parameters, all proton sources determine a unique equilibrium density, and the eigenvalues of the Jacobian matrix are always negative; all the equilibria are stable. In contrast, if only 0.1% of the outflowing protons are destroyed—the situation depicted in figure 11—then for a range of temperatures and sources there is no longer a one-to-one correspondence between proton source and equilibrium density, and unstable equilibria are possible. The Jacobian matrix has a positive eigenvalue.

Now we examine the effect of introducing H_2. Table 3 summarizes the physical parameters we use (d_{mol} is the fraction of molecules destroyed at the wall).

Γ_p	τ_p	τ_H	τ_{mol}	d_c	d_H	d_{mol}
1.489×10^{14} cm^{-3}s^{-1}	3 ms	1.3 μs	18.2 μs	0.01	10^{-4}	10^{-4}

Table 3.

If no molecules are involved, a *stable* recycling regime will be reached with a proton density of 10^{13} cm^{-3}. Protons and electrons flow into the plasma from the interior, and a source of neutral atomic H is recycled. We expect that small perturbations around this position will shift the position of the equilibrium by a small amount[6]. We shall examine the effect of increasing β, the fraction of H atoms which return associated into molecules, that is, we write

$$\begin{aligned} \Gamma_H^{\rm rec} &= (1-\beta)\Gamma_H^{\rm tot} \\ \Gamma_{\rm mol}^{\rm rec} &= \beta\Gamma_H^{\rm tot}/2 \end{aligned} \tag{36}$$

where $\Gamma_H^{\rm tot}$ is the total recycled source of H atoms, $\Gamma_H^{\rm rec}$ the source which re-enter the plasma as atoms, and $\Gamma_{\rm mol}^{\rm rec}$ = the source of molecules recycled into the plasma. We must also specify the vibrational state of the molecules as they enter the plasma, and we shall assume that they are either in their ground state (gs), or are excited, with a vibrational temperature of 3 eV.

Figure 12 gives an overview of the temporal behaviour of the plasma constituents as the fraction of recycled H_2 is changed. In each case a new equilibrium, characteristic of the recycled H_2 fraction is established. Extensive

[6]If the initial equilibrium were unstable, then small perturbations, such as the introduction of H_2 would cause a large change This is why we avoid starting from the (physically unrealistic) unstable situation depicted in figure 11

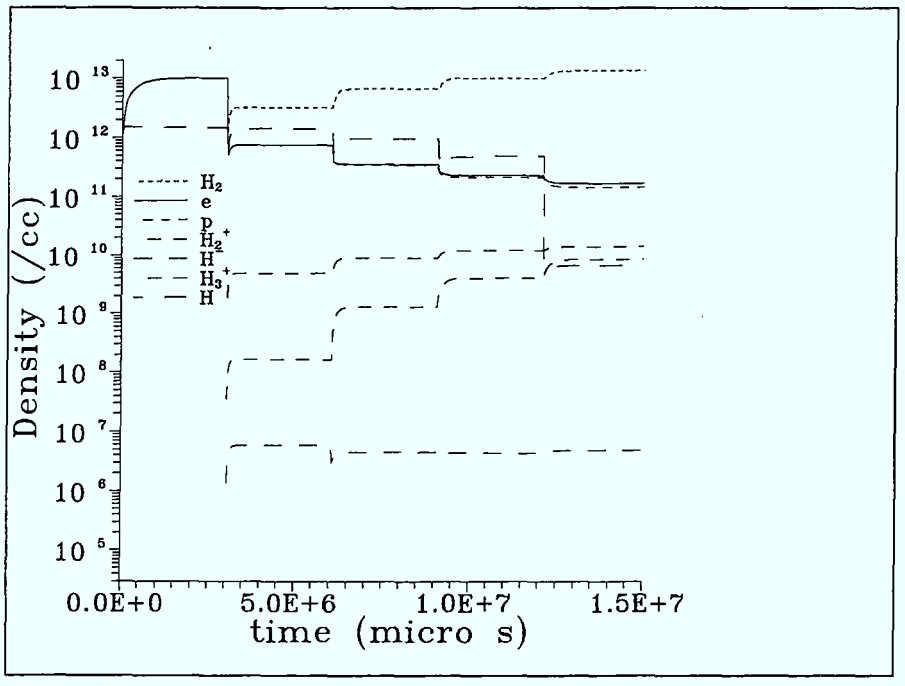

Figure 12. The approach to equilibrium. We show the temporal behaviour of the particle densities as a function of time for several values of β. All densities start from zero for each value of β. Molecules are recycled in their ground state, and the plasma temperature is 3 eV. The other parameters are given in table 3.

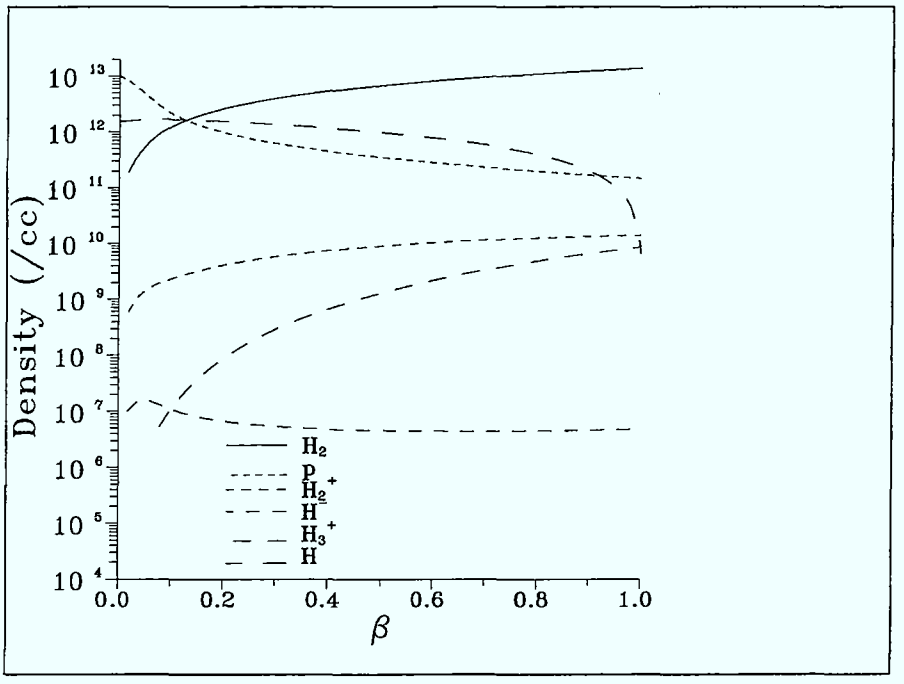

Figure 13. The equilibrium particle densities as a function of the molecular recycling fraction β. The parameters are given in table 3, and it is assumed that the H_2 enters the plasma in its ground vibrational state

calculations, which we do not present here, show that, for the parameters in table 3, the final equilibrium is independent of the starting conditions, and depends only on β, and, of course, the plasma parameters. In general this is not the case, and the final equilibrium depends on the starting conditions. We discuss this in the next section; here we present results for the case that the initial plasma density is zero. We consider two plasma temperatures, 3 eV and 8 eV, and two initial distributions of molecular vibrational states. In the first instance we assume that all the molecules are returned to the plasma in their ground vibrational state, and secondly, so that we can examine the effect of molecular excitation, we assume the recycled molecules have a vibrational temperature of 3 eV.

The behaviour of the plasma as a function of β, the fraction of particles recycled as H_2, is summarized in figures 13 and 14. Figure 13 shows how the particle concentrations at equilibrium vary as a function of β if the H_2 returns in its ground vibrational state, whereas figure 14 shows what happens if the molecules have a vibrational temperature of 3 eV. The greater efficacy of the excited state molecules is obvious.

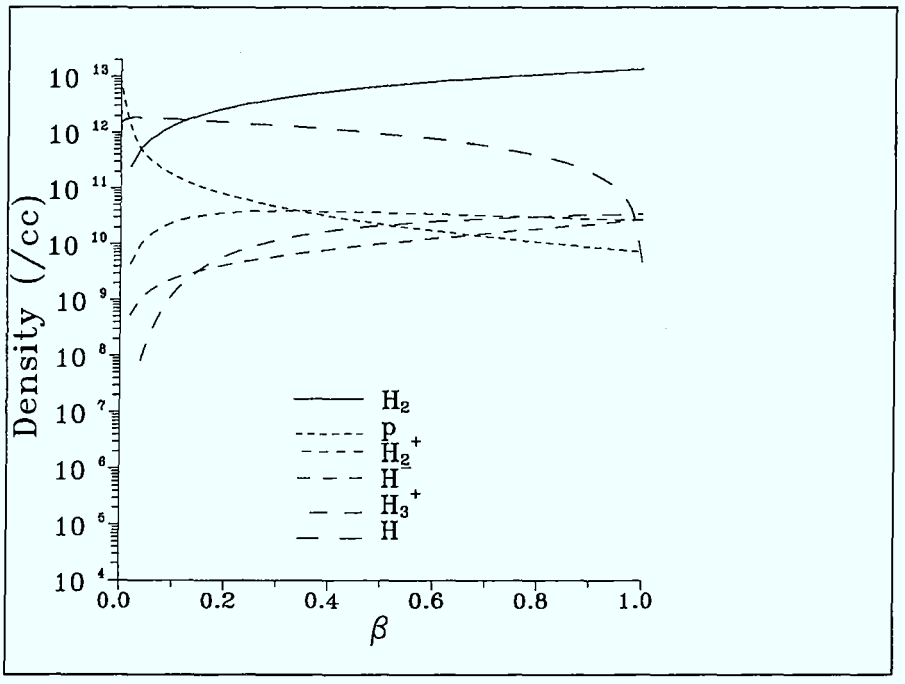

Figure 14. The equilibrium particle densities as a function of the molecular recycling fraction β. The parameters are given in table 3, and it is assumed that the H_2 enters the plasma with a vibrational temperature of 3 eV. Note its greater neutralization efficacy

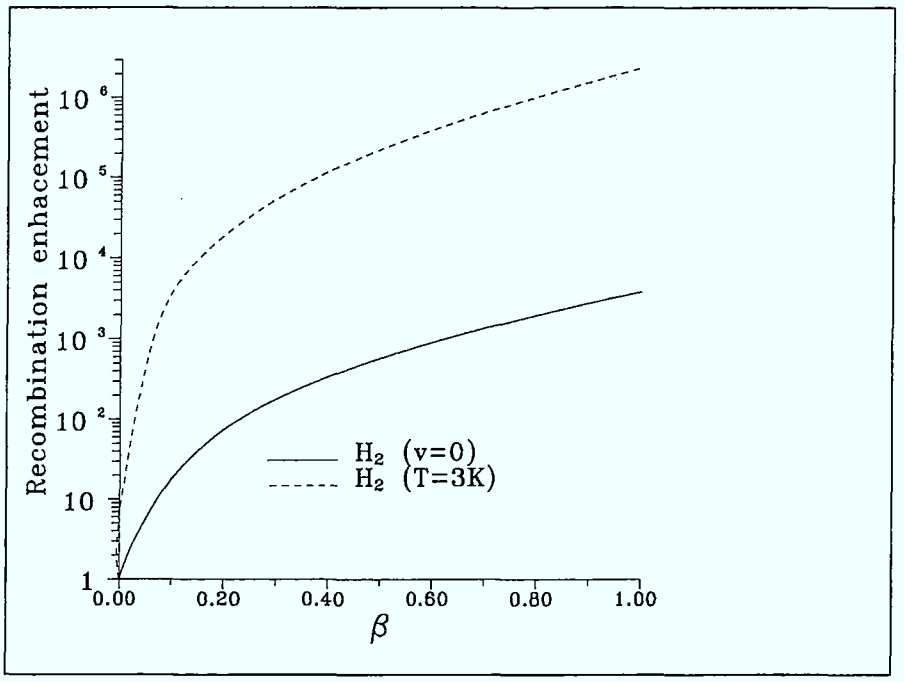

Figure 15. The enhancement in recombination as β varies for the parameters of table 3. The effect of vibrational enhancement is clear

Figures 13 and 14 show the situation when the plasma proton equilibrium density without H_2 recycling is $10^{13}\,\mathrm{cm}^{-1}$. Everything varies smoothly as a function of β, and even small amounts of H_2 cause a rapid neutralization, which we can characterize by giving α^{eff}, the effective recombination coefficient defined from equation 31a as

$$\alpha^{\mathrm{eff}} = \frac{\Gamma_p}{n_p^2} + S(n_e, T)\frac{n_0}{n_p} - \frac{1}{n_p \tau_p} \tag{37}$$

This is shown in figure 15. For the parameters considered here, the effective neutralization rate α^{eff} varies non-linearly with H_2 concentration. However, for small β, we may write, with α^0 the recombination rate in the absence of H_2

$$\alpha^{\mathrm{eff}} = \left[1 + \chi \frac{n_{H_2}}{n_p^0}\right] \alpha^0 \tag{38}$$

and can thus calculate an enhancement of the recombination which varies linearly with the concentration of H_2. We give some values in table 4 where we also give the maximum H_2 fraction for which equation 38 is valid. Graphs of the corresponding results are shown in figures 16 to 18.

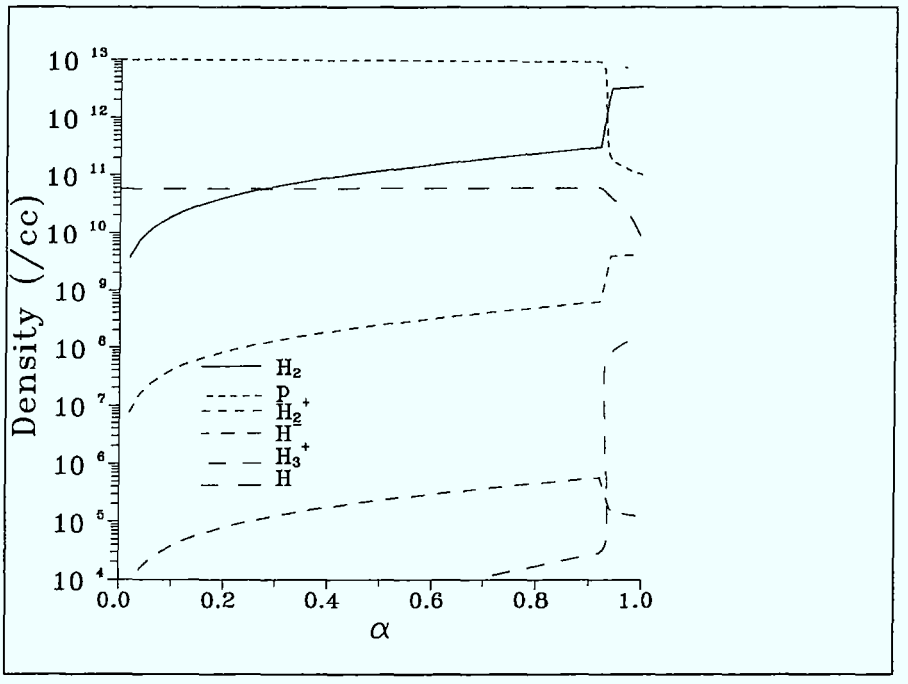

Figure 16. The equilibrium particle densities as a function of the molecular recycling fraction β. The parameters are given in table 3, except that the plasma temperature is 8 eV. It is assumed that the H_2 enters the plasma in its ground vibrational state The sudden jump at $\beta \sim 0.9$ is explained in the text

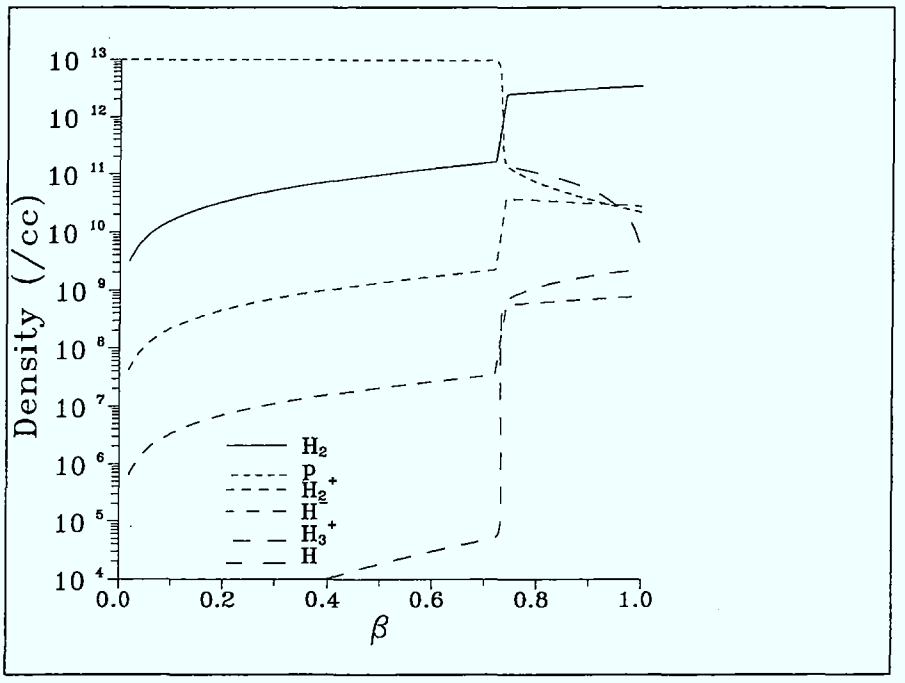

Figure 17. As for figure 16, but for a molecular vibrational temperature of 3 eV.

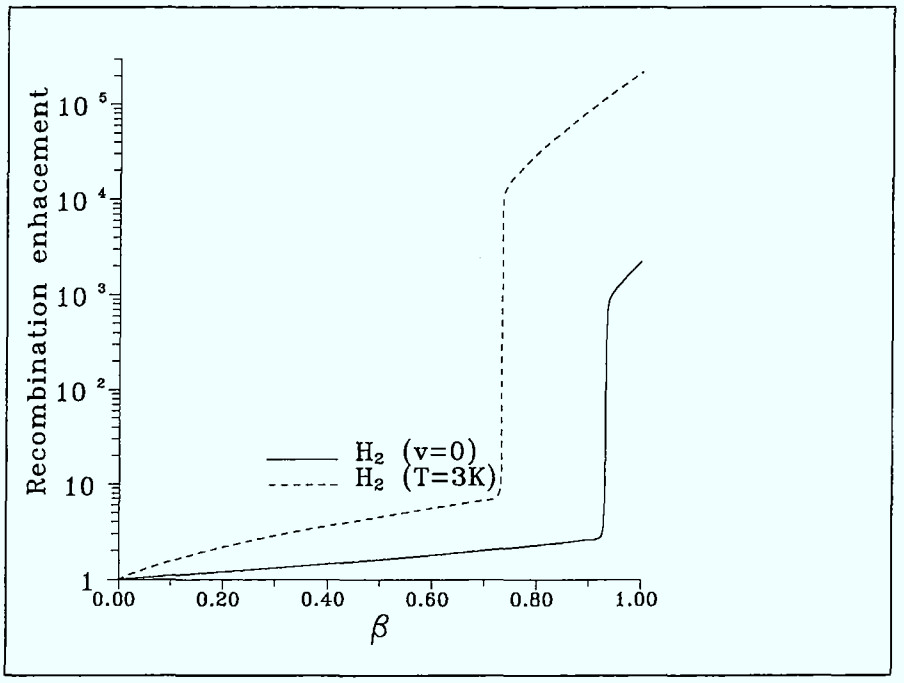

Figure 18. As for figure 15, but at a plasma temperature of 8 eV. Note the much smaller recombination enhancement for small β.

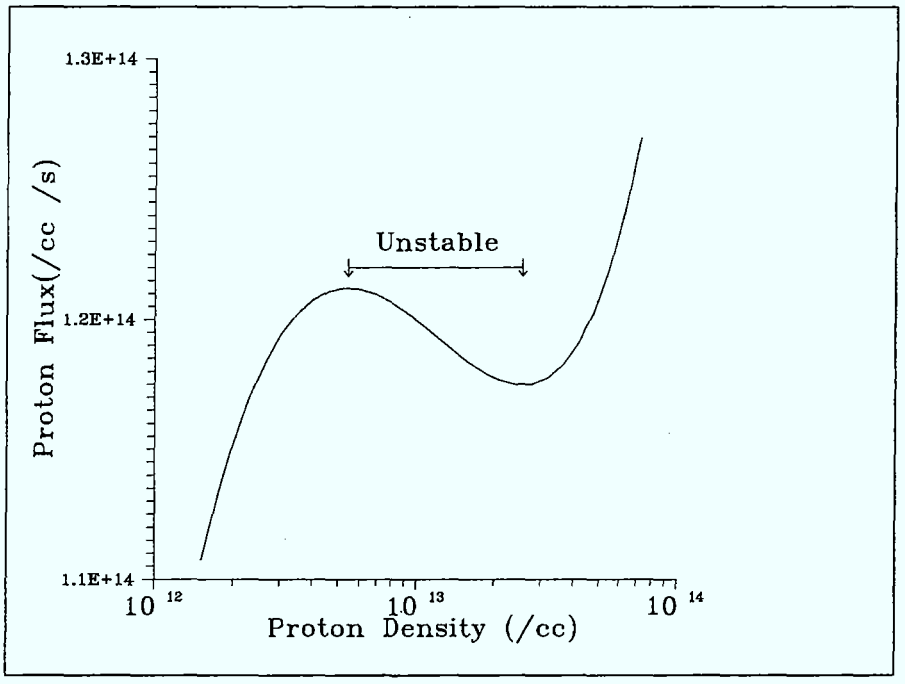

Figure 19. The relationship between proton source Γ_p and equilibrium density $n_p(\infty)$ for $d_c = 0.1\%$ and a plasma temperature of 3 eV. The region of instability is marked

However, as is clear from figures 16 to 18, H_2 recycling leads to instabilities as a function of β, and we consider these briefly in the next section.

	T=3 eV H_2(gs)	T=3 eV H_2^*	T=8 eV H_2(gs)	T=8 eV H_2^*
$n_p^0 = 10^{13}$	41	160	48	340
H_2^{max}	0.1	0.01	0.1	0.1
$n_p^0 = 10^{14}$	32	87	20	116
H_2^{max}	0.1	0.1	0.01	0.1

Table 4. χ values. H_2^{max} is the maximum value of n_{H_2}/n_p^0 for which equation 38 holds.

5. Instabilities

Figure 19[7] shows the relationship between proton source and equilibrium density (without H_2) at 3eV, if the proton destruction fraction is $d_c = 0.1\%$ The physical variable is the proton source Γ_p, and, as is clear from figure 19,

[7]This is a linear plot of the 3 eV result in figure 11.

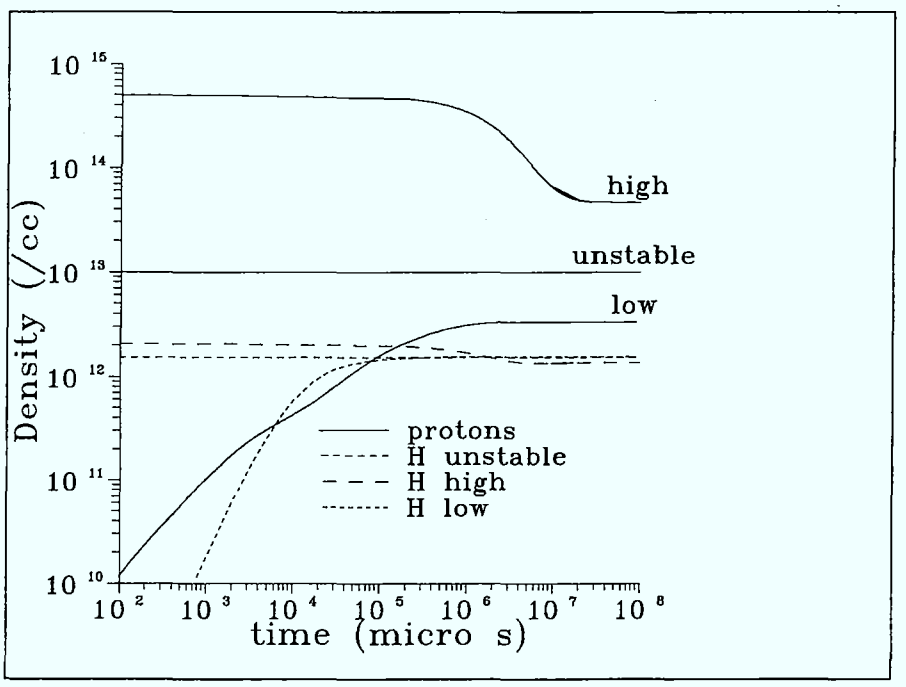

Figure 20. The approach to equilibrium. We show the proton and hydrogen density as a function of time for the parameters described in the text, and for three different starting conditions.

low all initial densities zero

high initial p and e densities 5×10^{14}, initial H density zero

unstable initial densities equal to final densities in the unstable case

if Γ lies between limits given by $1.175 \times 10^{14} < \Gamma_p < 1.212 \times 10^{14}$ $\mathrm{cm}^{-3}\mathrm{s}^{-1}$, then three equilibria can exist, two of which are stable, and one of which is not. Which solution is actually obtained depends on the initial conditions. We give an example in figure 20, which shows the temporal development of the proton (and therefore also electron), and hydrogen density, for different starting conditions. The proton source is set to be $\Gamma_p = 1.2 \times 10^{14}$, which implies that three final states are possible. They are summarized in table 5.

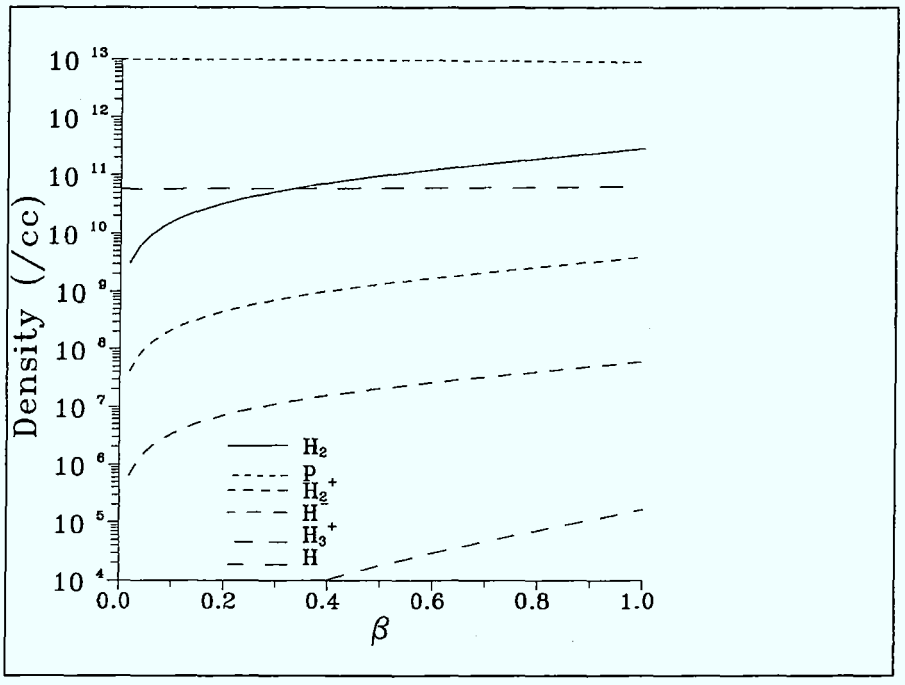

Figure 21. The equilibrium particle densities as a function of the molecular recycling fraction β. The parameters are given in table 3, except that the plasma temperature is 8 eV. It is assumed that the H_2 enters the plasma in its ground vibrational state. Here the initial proton density is 10^{14} cm^{-3}

	Low	Medium	High
$n_p(\infty)$	3.328×10^{12}	10^{13}	4.642×10^{14}
$n_0(\infty)/n_p(\infty)$	0.464	0.152	0.0292
ϵ_-	-1.60	+0.341	-0.209
	stable	unstable	stable

Table 5. ϵ_- is the largest eigenvalue of the Jacobian matrix.

Comparing figure 20 with table 5, we see that different starting conditions can indeed be found which lead to all three final equilibria. Very special conditions are needed to generate the unstable equilibrium, but the two stable equilibria, arise from initial low or high proton densities respectively. Thus, depending on the initial conditions, a fixed proton source can lead either to a high recycling regime, with a large neutral density and small proton density or to a low recycling regime with a high proton density and little hydrogen.

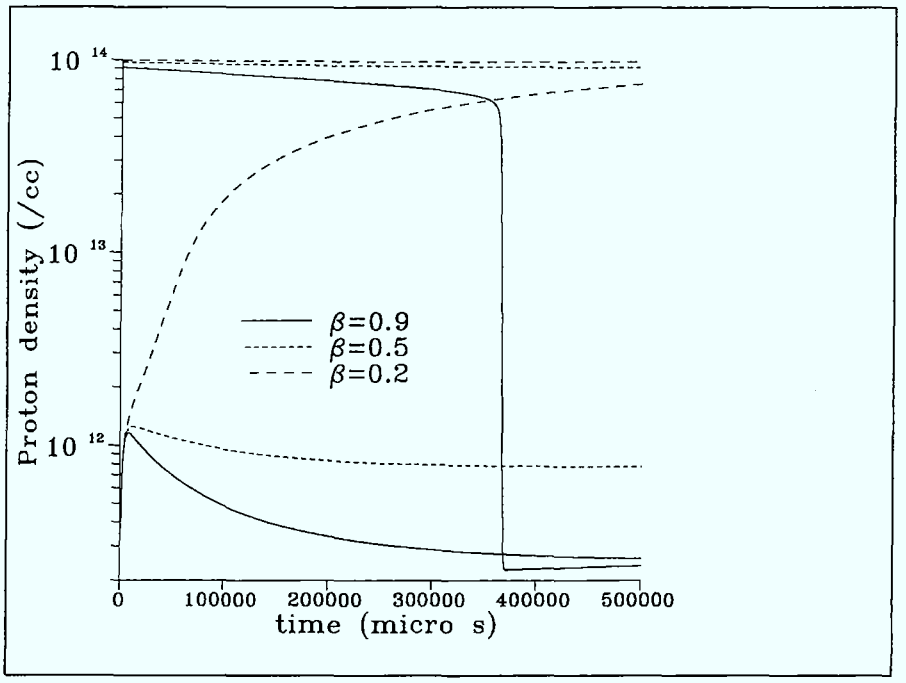

Figure 22. The approach of the proton density to equilibrium for various initial conditions and values of β. See text for further details

The situation is more complicated if H_2 recycling occurs. The recycling fraction β introduces an extra degree of freedom and it is clear that for a given starting condition, the final equilibrium also depends on β. This dependence is responsible for the sudden jumps as a function of β in figures 16 to 18. The value of β at which the jump occurs also depends on the starting conditions. In figure 21 we show the analogue of figure 17, but for a circumstance in which we assume that for each value of β the initial condition corresponds to the equilibrium without H_2 recycling. Since the two situations correspond to different physical processes—either the plasma is formed in the presence of molecules or is formed without them and then contaminated by their introduction—it is not surprising to find two different end results.

A plot similar to figure 20 makes the point. In figure 22 we show how the equilibrium proton densities develop as a function of time for different values of β and different initial conditions for the 3 eV high source case. For $\beta = 0.2$ the final equilibrium does not depend on the starting conditions, and is reached smoothly as a function of time. In contrast, for $\beta = 0.5$ the final equilibrium does depend on the initial density, but in each case is reached smoothly as a function of time. For high recycling, $\beta = 0.9$ the equilibrium does not depend on the initial density, but is only reached smoothly from

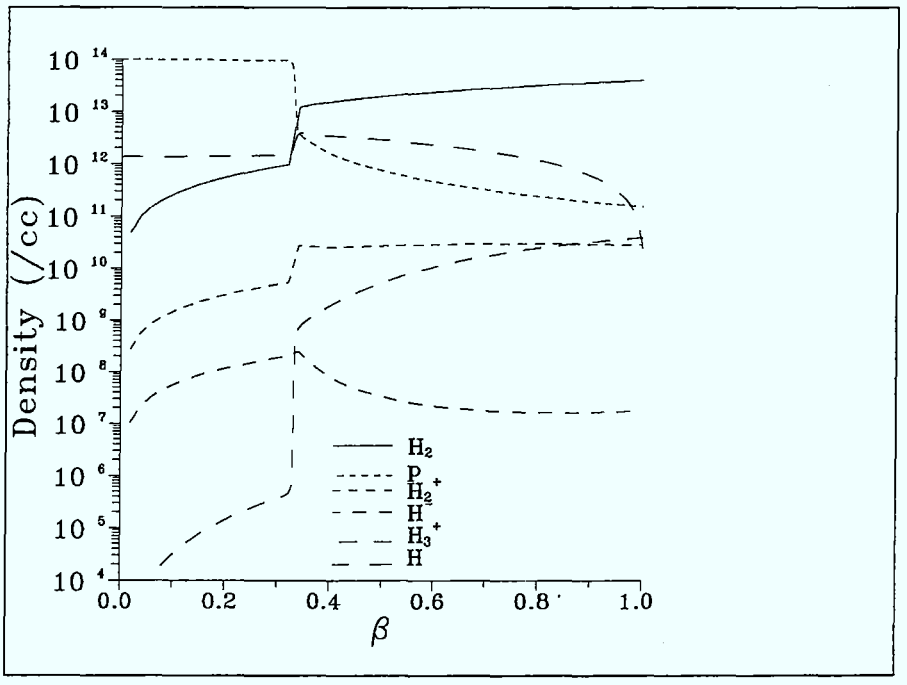

Figure 23. The equilibrium particle densities as a function of the molecular recycling fraction β. The parameters are given in table 3, except that the proton source $\Gamma = 4.357 \times 10^{14}$ cm^{-3}s^{-1}. This gives a proton density of 10^{14} cm^{-3} for $\beta = 0$. The initial plasma density is zero. The H_2 enters the plasma in its ground vibrational state

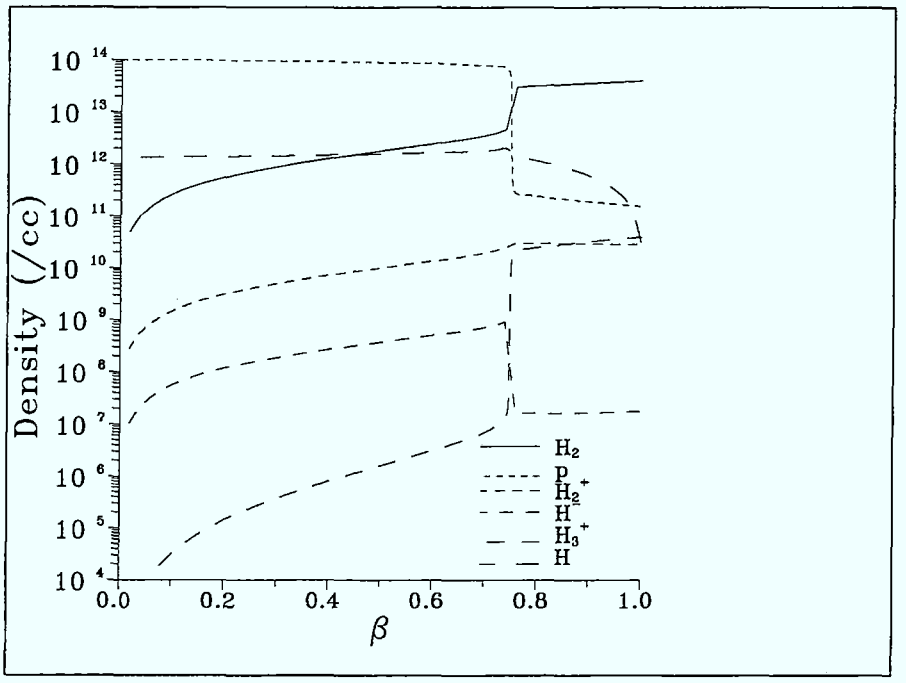

Figure 24. As for figure 23, but for an initial proton density of 10^{14} cm^{-3}, and corresponding H density

a low density start. If the initial density is high, then the proton density suffers a collapse, reminiscent of what was found in section 2. We do not discuss this further here, but note its potential for producing detachment. We conclude by giving further representative results in figures 23 to 26.

Summary

This report has considered some of the issues which must be addressed if molecular processes are important in plasmas. This is most likely to be the case near the plasma edge, where recycling is important.

A simple model treating ion conversion followed by dissociative recombination as molecular hydrogen streams into the plasma is too restrictive to be realistic, but, in spite of its non-linearity, can be solved analytically. It gives some useful insights; there is a time to come to vibrational equilibrium—$f \sim 6.5 \times 10^8/n_p$ s, where n_p is the proton density in cm^{-3}—and a much longer time t_0, which depends on the proton density and H_2 source, after which the proton density falls dramatically. This is to some extent an artifact of the model, which assumes that the neutral atomic hydrogen is removed from the system before it can be ionized, and so prevent the proton collapse. Nevertheless, the possibility that large sources of molecular hydrogen can

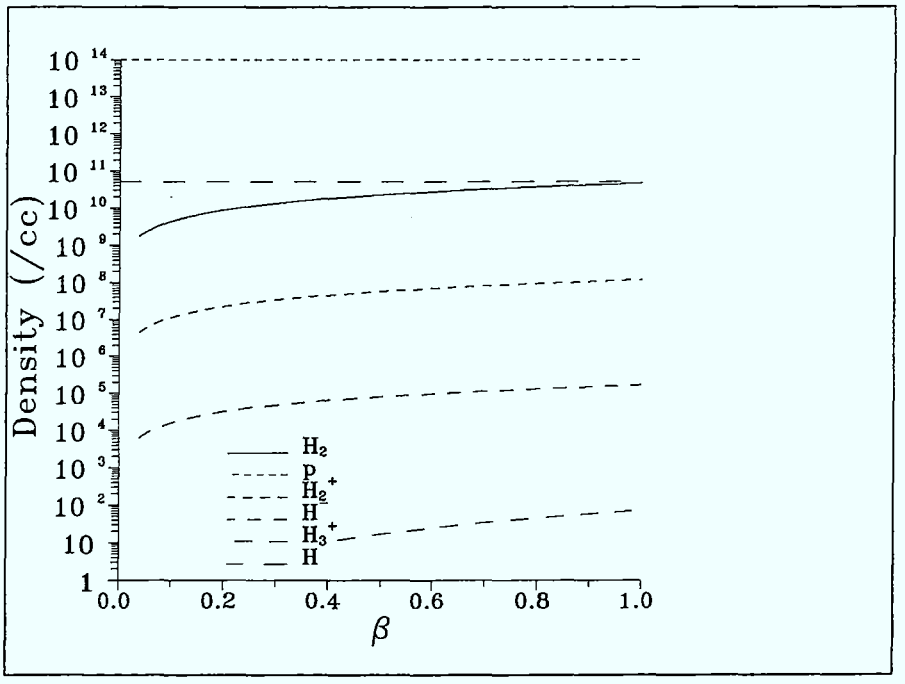

Figure 25. The equilibrium particle densities as a function of the molecular recycling fraction β. The parameters are given in table 3, except that the plasma temperature is 8 eV and the proton source $\Gamma = 3.372 \times 10^{14}$ cm^{-3}s^{-1}. This gives a proton density of 10^{14} cm^{-3} for $\beta = 0$. The initial plasma density is zero. The H_2 enters the plasma in its ground vibrational state

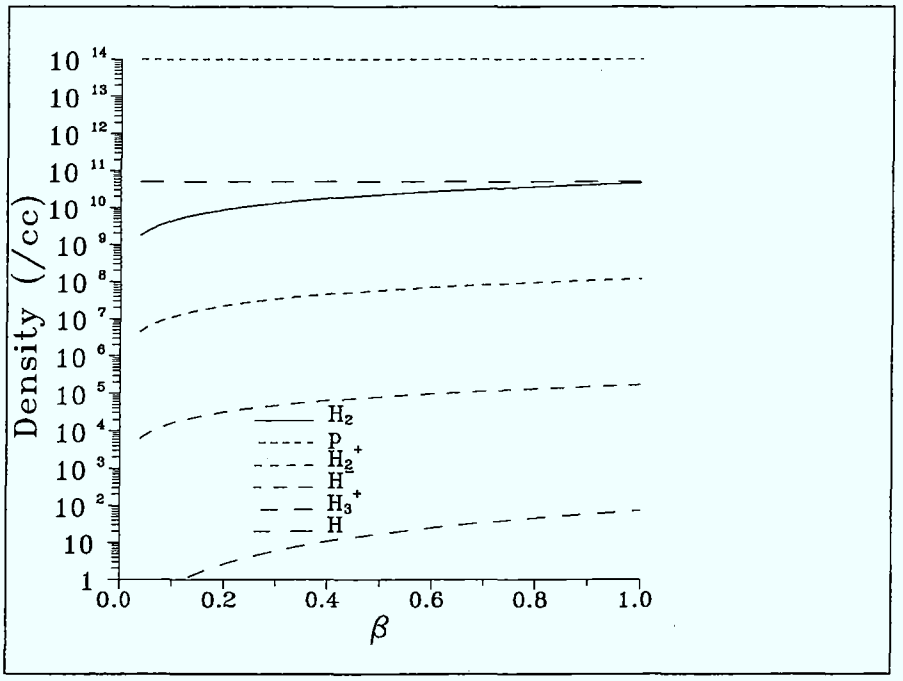

Figure 26. As for figure 25, but for an initial proton density of 10^{14} cm^{-3}

lead to dramatic non-linear effects cannot be ignored.

A more adequate model, which includes recycling by defining residence times for each species, and balances a source of plasma particles from the interior with loss terms has been solved numerically. It was found that as the concentration of molecules in the recycled particles increased so the recombination rate was enhanced, mainly due to ion conversion and dissociative recombination. The enhancement can be dramatic leading, in some circumstances, to an effective recombination rate many several orders of magnitude greater than what one expects in the absence of molecules. It has been suggested that high recombination rates enhance plasma detachment (Borrass 1995)

An important finding is that vibrationally excited molecules are more effective neutralizers. As table 4 shows, they seem to be relatively more effective at low density. This can be understood by considering their residence time τ_{mol}, which is shorter than their equilibration time at low density, but comparable at higher densities. Thus, at low density the molecular state is strongly dependent on its vibrational state as it enters the plasma; this is less the case for higher plasma density. We have not explored this in great detail here.

The implication of this observations that the electron vibration-vibration transition rates between excited states are likely to be more important at

high densities, since they are significant in altering the vibrational state of the incoming molecules. At all energies the ion conversion cross section for charge transfer from vibrationally excited states and the inverse process are important and not well known. Their measurement, or calculation at eV temperatures is probably the most urgently needed piece of atomic data. We have not treated electronically excited molecules, nor have we included vibrational or electronic excitation of H_2^+, and so are unable to estimate the importance of these processes. We should point out that, unlike atoms, there is a strong isotope effect in molecules. The molecules of interest in fusion plasmas are D_2, T_2 and DT all of which have different vibrational spectra and cross sections. Data for H_2 is not enough.

Finally we considered a set problems connected with the non-linearity of our equations. It is difficult to know how strongly the instabilities we discuss depend on our specific model, but they do suggest that care is needed. If they persist in more adequate models, they suggest that molecules may be important in producing detachment in high density edge plasmas.

We close with a warning. We have already noted the slow timescale for vibrational change. This makes it unlikely that a collisional-radiative model in which vibrational excitation is assumed to be a fast process will be successful. This view is reinforced by the observation that a CR model is intrinsically linear. Many of the phenomena we find to be characteristic of molecular processes are non-linear.

Acknowledgements

We have enjoyed useful conversations with D Post and M Bacal.

References

Abramowitz M, Stegun IA (1970): 'Handbook of Mathematical Functions', Dover (New York).

Bardsley JN, Wadehra JM (1979): Phys Rev **A20**,1398.

Borrass K (1995):'Study of the rôle of recombination in detachment', ITER Expert group meeting Naka.

Janev RK, Langer WD, Evans Jr K, Post Jr DE (1987) 'Elementary processes in hydrogen-helium plasmas' Springer-Verlag (Berlin).

Janev RK, Post DE, Langer WD, *et al* (1984) J. Nucl Mat **121**, 10.

Krasheninnikov SI, Pigarov AYu and Sigmar DJ (1996): Phys Lett **A214**, 285.

Rescigno TN, Schneider BI (1988): J. Phys. B (At. Mol. Phys) **21**, L691.

Sawada K, Fujimoto T (1995): J. Appl Phys **78**, 2913.

Appendix 1

This appendix records the atomic data actually used in the codes. Most of the rates are taken from Janev *et al* (1987), augmented with some extra results. Table A1 shows which rates are presently programmed from Janev's fits. Those marked → are included in our code. The processes marked † also have scaling laws based on data for cross sections of vibrationally excited states. The actual laws used are recorded below.

There is a complication for heavy particle collisions. Janev *et al* tabulate rates for fixed heavy projectiles with fixed velocity traversing a target of given temperature, whereas we require the rates for the circumstance in which both projectile and target have effective temperatures. However it is not difficult to show that

$$S_2(T_1, T_2) = S_1(T_{\rm eff}) = < \sigma v >_{V \to 0} (T_{\rm eff}) \qquad (A1.1)$$

where $S_2(T_1, T_2)$ is the rate coefficient for collisions between particles of type 1 at temperature T_1 and particles of type 2 at temperature T_2, $S_1(T_{\rm eff})$ is the rate coefficient for stationary particles of type 2 in a bath of particles of type 1 at temperature $T_{\rm eff}$, and $< \sigma v >_V (T)$ is the quantity tabulated by Janev *et al*, that is the rate coefficient for collisions between particles of type 1 at temperature T in collision with a beam of particles of type 2 with velocity V. We have

$$T_{\rm eff} = \frac{M}{M_1} T_1 + \frac{M}{M_2} T_2 \qquad (A1.2)$$

where M_1 and M_2 are the masses of particles of types 1 and 2 respectively, and M is the mass of the target particles[8] used in preparing the tables of $< \sigma v >_V (T)$. In the table below the 'particle of type 1' is always listed *first* in the description of the reaction, so that t_r, the correction factor, defined so that the correct rate coefficient to use for the reaction is

$$S = < \sigma v >_{V \to 0} [(1 + t_r)T] \qquad (A1.3)$$

is given by M_1/M_2. In equation 2 T is the plasma temperature; I assume that the heavy particles have the same temperature. (If the heavy particles are assumed to be stationary, as is always effectively the case with heavy particles in an electron bath at temperature T, then $t_r = 0$.) Notice that *except for rate 18* we always have $t_r \leq 1$. In fact, the smallest value of V given by Janev *et al*'s tabulation corresponds to a heavy particle energy of 0.1 eV. At present, our tabulation uses a value of 0.37 eV.

Scaling laws:

[8] *ie* those particles whose velocities are assumed to be thermally distributed in the tabulation of $< \sigma v >_V (T)$, that is, particles of type 1 as described here

For process 1

$$S_{k(>v)\leftarrow v} = \frac{e^{[5E_v - 4.44E_k]}}{0.121} S_{1\leftarrow 0} \qquad (A1.4)$$

based on a fit to cross section data from Bardsley and Wadehra (1979). The rate $S_{k(<v)\leftarrow v}$ is obtained by detailed balance.

For process 6

$$S_v = \frac{e^{-0.07E_v}}{1.0019} S_0 \qquad (A1.5)$$

based on cross section data from Rescigno and Schneider(1988).

For process 13

$$S_v = \frac{3.36S_0}{0.0202 + (2.1 - E_v)^2} \qquad (A1.6)$$

based on a Lorenzian designed to give a total capture cross section equal to the $H - H^+$ resonant charge transfer cross section at zero energy defect.

In the above formulae, E_v is the *excitation* energy, in eV of the state with vibrational quantum number v (including the zero point energy), given by

$$E_v = 0.545666(v + \frac{1}{2}) - 0.015044(v + \frac{1}{2})^2 \qquad (A1.7)$$

and S_0 ($S_{1\leftarrow 0}$) is the rate for the process in the ground vibrational state given by Janev *et al.* S_v ($S_{k(>v)\leftarrow v}$) is the rate for the corresponding process starting in the vibrational level v.

Dissociative Attachment

The rate coefficients for processes

$$e + H_2(v) \rightarrow H^- + H$$

have been fitted to a simple analytic form, based on a fit to the cross sections of Bardsley and Wadehra (1979): *viz*

$$S_v(T) \sim 6.69 \times 10^7 \sigma_v^{\text{thresh}} \sqrt{T} \frac{1 + (\alpha T + 1)\frac{E_v}{T}}{(1 + \alpha T)^2} \exp\{-E_v/T\} \qquad (A1.8)$$

where $S_v(T)$ is the rate coefficient ($cm^3 s^{-1}$ at temperature T (eV), E_v is the *threshold* energy (in eV) for dissociative attachment from the v'th vibrational level, and σ_v^{thresh} is the corresponding threshold cross section (in cm^2). The parameter α has the mean value

$$\alpha \sim 2.27 \ \ (\text{eV})^{-1}$$

In fact, each vibrational level has its own value of α, and these, together with the threshold cross sections and energies are shown below.

State v	1	2	3	4	5
σ_{thresh}	2.5^{-21}	1.3^{-19}	1.3^{-18}	8.9^{-18}	5^{-17}
α	1.66	2.37	2.06	2.36	2.35
E_v	3.763	3.237	2.763	2.316	1.868
State v	6	7	8	9	10
σ_{thresh}	1.6^{-16}	4.5^{-16}	4^{-16}	3.2^{-16}	4.5^{-16}
α	2.29	2.32	2.21	2.27	2.15
E_v	1.474	1.079	0.737	0.421	0.132

The threshold cross sections cm^2
and energies (eV) for the first 10 states
in H_2, and the values of α (eV^{-1})
a^b means $a \times 10^b$.

Expression 1 agrees with what was given by Wadehra at the IAEA meeting on molecular processes, and the DA rates calculated with it and the values tabulated above agree with results by Biel of Düsseldorf (private communication).

We also include the processes

$$H^- + H_2^+ \rightarrow H + H_2$$

and

$$H^- + H_3^+ \rightarrow 2H_2$$

for which we assume a velocity independent cross section of 1.5×10^{-14} cm^2 (B.Peart, private communication)

We derive a rate for the inverse of ion conversion (rate 13 below) from detailed balance as

$$S(H_2^+ + H \rightarrow p + H_2) = \frac{1}{2} \exp[1.83/T] S_v(H_2 + p \rightarrow H + H_2^+)$$

where $S_v(H_2 + p \rightarrow H + H_2^+)$ is the rate for ion conversion obtained from our scaling law. We make no correction for the change in energy defect when excited molecules are involved.

Finally, all the rates for atomic hydrogen are taken from Sawada and Fujimoto (1995).

The Janev Data

Index	Section	$M_1 + M_2 \rightarrow$ products	process	t_r
$\rightarrow$ †1	2.2.1a	$e+H_2(v=0) \rightarrow e+H_2(v=1)$	vib excitation $\Delta v = 1$	0
$\rightarrow$ 2	2.2.1b	$e+H_2(v=0) \rightarrow e+H_2(v=2)$	vib excitation $\Delta v = 2$	0
3	2.2.2	$e+H_2 \rightarrow e+H_2^*$	electronic excitation	0
4	2.2.3	$e+H_2 \rightarrow e+H_2^*$	electronic excitation	0
5	2.2.4	$e+H_2 \rightarrow e+H_2^*$	electronic excitation	0
$\rightarrow$ †6	2.2.5	$e+H_2 \rightarrow e+H+H$	impact dissociation (Diss)	0
7	2.2.6	$e+H_2 \rightarrow e+H+H^*$	impact dissociation	0
8	2.2.7	$e+H_2 \rightarrow e+H^*+H^*$	impact dissociation	0
9	2.2.8	$e+H_2 \rightarrow e+H+H^*$	impact dissociation	0
$\rightarrow$ 10	2.2.9	$e+H_2 \rightarrow e+H_2^+ +e$	ionization	0
11	2.2.10	$e+H_2 \rightarrow e+H^+ +H+e$	ionization+dissociation	0
12	3.2.2	$p+H_2(v=0) \rightarrow p+H_2(v>0)$	proton vibrational excitation	0.5
$\rightarrow$ †13	3.2.3	$p+H_2 \rightarrow H(1s)+H_2^+$	ion conversion (IC)	0.5
14	3.2.4a	$p+D_2 \rightarrow D^+ +HD$ (or H+D)	p–d exchange	0.25
15	3.2.4b	$p+D_2 \rightarrow D+HD^+$	p–d exchange	0.25
16	3.2.5	$p+H_2 \rightarrow p+H_2^+(v \leq 9)+e$	proton impact ionization	0.5
17	3.2.6	$p+H_2^+ \rightarrow p+H(1s)+H^+$	proton impact dissociation	0.5
18	4.2.1	$H_2^+ +H(1s) \rightarrow H^+ +H+H(1s)$	hydrogen impact dissociation	2.0
19	7.2.1	$p+H^- \rightarrow p+H+e$	proton impact detachment	1.0
$\rightarrow$ 20	7.2.2	$p+H^- \rightarrow H^*(n=2)+H(1s)$	mutual neutralization (MN)	1.0
$\rightarrow$ 21	7.2.3	$p+H^- \rightarrow H^*(n=3)+H(1s)$	mutual neutralization	1.0
22	7.3.1	$H^- + H(1s) \rightarrow H(1s)+H^-$	charge exchange	1.0
23	7.3.2a	$H^- +H \rightarrow H+H+e$	hydrogen impact detachment	1.0
24	7.3.2b	$H^- +H \rightarrow H_2+e$	associative detachment	1.0
25	2.2.11	$e+H_2^+ \rightarrow e+H^+ +H^+ +e$	breakup	0
$\rightarrow$ 26	2.2.12	$e+H_2^+ \rightarrow e+H^+ +H(1s)$	dissociation	0
$\rightarrow$ 27	2.2.13	$e+H_2^+ \rightarrow e+H^+ +H^*(n=2)$	dissociation	0
$\rightarrow$ 28	2.2.14	$e+H_2^+ \rightarrow H(1s)+H^*(n)$	dissociative recombination (DR)	0
$\rightarrow$ 29	7.1.1	$e+H^- \rightarrow e+H(1s)+e$	electron impact detachment (Det)	0
30	7.1.2	$e+H^- \rightarrow e+H^+ +2e$	detachment and ionization	0
31	2.1.8	$e+H^+ \rightarrow H^*(n) + h\nu$	radiative recombination	0
$\rightarrow$ 32	2.2.15(a/b)	$e+H_3^+ \rightarrow 3H/H_2+H^*$	H_3^+ neutralization	0
$\rightarrow$ 33	2.2.16	$e+H_3^+ \rightarrow e+H^+ + 2H$	H_3^+ breakup	0
$\rightarrow$ 34	4.3.3	$H_2^+ + H_2 \rightarrow H_3^+ + H$	H_3^+ production	1.0
$\rightarrow$ 35	7.3.2a	$H^- + H \rightarrow H+H+e$	H impact dissociation	1.0
$\rightarrow$ 36	7.3.2a	$H^- + H \rightarrow H_2 + e$	associative detachment	1.0

Appendix 2

We give details of the analytic solutions presented in section 2. Our starting point is equation 9 of the text, which we reproduce here.

$$\dot{y} = y(Z'(t) - Ay) \tag{A2.1}$$

It is straightforward to verify that its solution is given by

$$y(t) = \frac{y_0 F'(t)}{1 + y_0 A F(t)} \tag{A2.2}$$

where

$$F(t) = \int_0^t \exp[Z(t')]\ dt' \tag{A2.3}$$

and

$$Z(t) = \int_0^t Z'(t')\ dt' \tag{A2.4}$$

and, of course $y_0 = y(0)$. Applying this to equation 8 gives equation 12 of the text. Charge conservation (equation 6d) implies

$$\dot{n}_e = S_{DR}[n_p(t) - n_e] \tag{A2.5}$$

which is also of the form A2.1, since we know $n_p(t)$. However, the exact solution requires

$$Z(t) = \int_0^t n_p(t')\ dt'$$

which is too complex to be useful. The integral can be done if the asymptotic form for n_p (equation 23a) is used. This gives

$$n_e(t) = \frac{n_0 \exp[-(\alpha' - \beta' t)^2](\alpha' - \beta' t)^{-\lambda}}{e^{-\alpha'^2}\alpha'^{-\lambda} + \alpha'\{\gamma[q, \alpha'^2] - \gamma[q, (\alpha' - \beta' t)^2]\}} \tag{A2.6}$$

where

$$\begin{aligned} \alpha' &= \sqrt{S_{DR}/2\Gamma}\, n_0 \\ \beta' &= \sqrt{S_{DR}\Gamma/2} \\ \lambda &= S_{DR}/S_p \end{aligned}$$

and $\gamma[q, z]$ is an incomplete γ function (Abramowitz and Stegun 1970). (Notice that setting $\lambda = 0$ and making appropriate modifications to α' and β' recovers the proton density result, because $\gamma[\frac{1}{2}, z^2] = \sqrt{\pi}\mathrm{erfc}(z)$.)

Equation A2.6 is only valid in the asymptotic region 1 (equation 23a). Expanding to the same order as 23a finally gives equation 24 for the electron (and hence also H_2^+) density in region 1.

Finally, 'long' after the proton collapse we may solve for the electron and H_2^+ density as they recombine (once again using A2.1 and A2.2). Now, however, we must specify a time t_1 and corresponding electron density n_1 appropriate to 'long' after the protons have disappeared. This is not very well defined, but by assuming that the H_2^+ density is symmetric in time about t_0, the proton collapse time, and estimating the duration of the proton collapse as being $\delta t \sim 1/2\beta$ we arrive at the, admittedly not very good estimates

$$t_1 \sim t_0 + \frac{1}{2\beta}$$

$$n_1 \sim \frac{2\beta}{S_{DR}}$$

Appendix 3

We consider only the atomic hydrogen. Its equation of motion is

$$\begin{bmatrix} \dot{n}_0 \\ \dot{n}_p \\ \dot{\mathbf{n}}_x \end{bmatrix} = \begin{bmatrix} M_0 & r_0 & \mathbf{h} \\ S_0 & -R & \mathbf{S} \\ \mathbf{v} & \mathbf{r} & \mathbf{M}_x \end{bmatrix} \begin{bmatrix} n_0 \\ n_p \\ \mathbf{n}_x \end{bmatrix} - \rho \begin{bmatrix} n_0 \\ n_p \\ \mathbf{n}_x \end{bmatrix} + \begin{bmatrix} \Gamma_{rec} \\ \Gamma_p \\ \mathbf{\Gamma}_x \end{bmatrix} \qquad (A3.1)$$

where n_0 is the hydrogen ground state density, n_p the proton density and $\mathbf{n}_x$ is a vector of excited state hydrogen densities. The coupling matrix has been set out in an obvious notation. $\mathbf{M}_x$ is a $N_x \times N_x$ matrix, where N_x is the number of excited hydrogen states the other bold-faced quantities are either $1 \times N_x$ ($\mathbf{h}$, $\mathbf{S}$) or $N_x \times 1$ ($\mathbf{v}$, $\mathbf{r}$) matrices. ρ is a diagonal matrix whose k'th diagonal element is the inverse of the residence time for species k , *ie*

$$\rho = \mathrm{diag}\{\frac{1}{\tau_H}, \frac{1}{\tau_p}, \frac{1}{\tau_H}, \cdots, \frac{1}{\tau_H}\} \qquad (A3.2)$$

$\mathbf{\Gamma}_x$ is a source term of excited state H which is formed externally, for example by molecular processes.

An important feature of the coupling matrix as we have written it is that all its columns add to zero. We shall make use of this later.

A collisional radiative model is usually derived by assuming that the excited state populations come to equilibrium much more rapidly than any other timescale in the problem, so that it is a good approximation to write

$$\dot{\mathbf{n}}_x = \mathbf{0} \qquad (A3.3)$$

and to solve the resulting algebraic equations for $\mathbf{n}_x$ in terms of n_0, n_p *etc.* Substituting these equations into A3.1 then leads to effective rate equations for only the slowly varying components. Doing this gives

$$\mathbf{n}_x = -\left\{[\mathbf{M}^{-1}\mathbf{v}]n_0 + [\mathbf{M}^{-1}\mathbf{r}]n_p + \mathbf{M}^{-1}\mathbf{\Gamma}_x\right\} \qquad (A3.4)$$

where the matrix $\mathbf{M}$ *is derived from* $\mathbf{M}_x$ *by subtracting the excited state residence times from the diagonal, so that, in an obvious notation*

$$\mathbf{M} = \mathbf{M}_x - \mathrm{diag}\{\frac{1}{\tau_H}, \cdots\} \qquad (A3.5)$$

From this we derive our CR equations.

$$\begin{bmatrix} \dot{n}_0 \\ \dot{n}_p \end{bmatrix} = \begin{bmatrix} M_0 - \mathbf{h}\mathbf{M}^{-1}\mathbf{v} - \frac{1}{\tau_H} & r_0 - \mathbf{h}\mathbf{M}^{-1}\mathbf{r} \\ S_0 - \mathbf{S}\mathbf{M}^{-1}\mathbf{v} & -R - \mathbf{S}\mathbf{M}^{-1}\mathbf{r} - \frac{1}{\tau_p} \end{bmatrix} \begin{bmatrix} n_0 \\ n_p \end{bmatrix} + \begin{bmatrix} \Gamma_0^{CR} \\ \Gamma_p^{CR} \end{bmatrix} \qquad A3.6$$

with

$$\begin{bmatrix} \Gamma_0^{CR} \\ \Gamma_p^{CR} \end{bmatrix} = \begin{bmatrix} \Gamma_{rec} - \mathbf{h}\mathbf{M}^{-1}\mathbf{\Gamma}_x \\ \Gamma_p - \mathbf{S}\mathbf{M}^{-1}\mathbf{\Gamma}_x \end{bmatrix} \qquad (A3.7)$$

where the total recycled source Γ_{rec} is given by

$$\Gamma_{rec} = \frac{1-d_c}{\tau_p} n_p + \frac{1-d_H}{\tau_H}(n_0 + n_{tot}) \qquad (A3.8)$$

Now n_{tot} is the total excited state population, which, from equation A3.4 is given by

$$n_{tot} = \sum_k \mathbf{n}_{xk} = -\sum_k \left\{ [\mathbf{M}^{-1}\mathbf{v}] n_0 + [\mathbf{M}^{-1}\mathbf{r}] n_p + \mathbf{M}^{-1}\mathbf{\Gamma}_x \right\}_k \qquad (A3.9)$$

where the sum k runs over all the excited states.

Now, if, as is usual, $\mathbf{M}_x$, rather than $\mathbf{M}$ had been used in the above equations, then the circumstance that the column sums of the original coupling matrix are all zero would imply that the column sums in the CR matrix (A3.6) are also zero. Thus, adding the columns in A3.6 gives

$$\dot{n}_0 + \dot{n}_p = \Gamma_p - \frac{d_c}{\tau_p} - \frac{d_H}{\tau_H} + \frac{1-d_H}{\tau_H} n_{tot} + \sum_k \Gamma_{xk} \qquad (A3.10)$$

where we have also used the result, once again derivable from the zero value of the column sums, that for any vector $\mathbf{q}$

$$-\sum_k \left\{ \left[\mathbf{h}\mathbf{M}_x^{-1} + \mathbf{S}\mathbf{M}_x^{-1} \right] \mathbf{q} \right\}_k = \sum_k q_k \qquad (A3.11)$$

The situation is significantly different if $\mathbf{M}$ rather than $\mathbf{M}_x$ is used. It is convenient to define

$$\bar{v} = -\sum_k [\mathbf{M}^{-1}\mathbf{v}]_k \qquad (A3.12)$$

and

$$\bar{r} = -\sum_k [\mathbf{M}^{-1}\mathbf{r}]_k \qquad (A3.13)$$

It is then straightforward to show that

$$M_0 - \mathbf{h}\mathbf{M}^{-1}\mathbf{v} + S_0 - \mathbf{S}\mathbf{M}^{-1}\mathbf{v} = -\frac{\bar{v}}{\tau_H} \qquad (A3.14)$$

and

$$r_0 - \mathbf{h}\mathbf{M}^{-1}\mathbf{r} - R - \mathbf{S}\mathbf{M}^{-1}\mathbf{r} = -\frac{\bar{r}}{\tau_H} \qquad (A3.15)$$

Furthermore equation A3.11 becomes

$$-\sum_k \left\{ \left[\mathbf{h}\mathbf{M}^{-1} + \mathbf{S}\mathbf{M}^{-1} + \frac{1}{\tau_H}\mathbf{M}^{-1} \right] \mathbf{q} \right\}_k = \sum_k q_k \qquad (A3.16)$$

But, as we see from equation A3.4 $-\sum_k [\mathbf{M}^{-1}\mathbf{\Gamma}_x]_k$ is just the total excited state equilibrium population attributable to the external process represented by $\mathbf{\Gamma}_x$. Furthermore, as is clear from equations A3.11 and A3.12 $\bar{v}n_0$ and $\bar{r}n_p$ are the total excited state populations held in CR equilibrium with the hydrogen ground state and ions respectively.

Taking these corrections into account we see that equation A3.10 becomes

$$\dot{n}_0 + \dot{n}_p = \Gamma_p - \frac{d_c}{\tau_p}n_p - \frac{d_H}{\tau_H}n_0 - \frac{d_H}{\tau_H}n_{tot} + \sum_k \Gamma_{xk} \qquad (A3.17)$$

which we may write as

$$\dot{n}_0 + \dot{n}_p = \Gamma_p - \frac{d_c^{\text{eff}}}{\tau_p}n_p - \frac{d_H^{\text{eff}}}{\tau_H}n_0 + \sum_k \Gamma_{xk} + \frac{d_H}{\tau_H}\sum_k \left[\mathbf{M}^{-1}\mathbf{\Gamma}_x\right]_k \qquad (A3.18)$$

where

$$d_c^{\text{eff}} = d_c + \frac{d_H \tau_p \bar{r}}{\tau_H} \qquad (A3.19)$$

and

$$d_H^{\text{eff}} = d_H(1 + \bar{v}) \qquad (A3.20)$$

These results have a very obvious interpretation. Since it is basic to any CR model that $\dot{n}_{tot} = 0$, the left hand side of either equation A3.10 or A3.17 is the rate of change of total proton density. Equation A3.17 correctly gives this change as the difference between the total source $(\Gamma_p + \sum_k \Gamma_{xk})$ and total sink $(n_p d_c/\tau_p + n_0 d_H/\tau_H + n_{tot} d_H/\tau_H)$, whereas equation A3.10 adds a spurious source of strength n_{tot}/τ_H, because basing the CR model on $\mathbf{M}_x$ allows for the production of protons through the recycling of excited state atoms, but, because their removal from the plasma is not properly treated, their loss is underestimated.

The quantity n_{ex} defined in the text is, of course, given by

$$n_{ex} = \bar{v}n_0 + \bar{r}n_p \qquad (A3.21)$$

since there is no contribution to the excited states from $\mathbf{\Gamma}_x$. The coefficients S and α used in the text are given by

$$S = S_0 - \mathbf{S}\mathbf{M}^{-1}\mathbf{v} \qquad (A3.22)$$

and

$$\alpha = +R + \mathbf{S}\mathbf{M}^{-1}\mathbf{r} \qquad (A3.23)$$

FORSCHUNGSZENTRUM JÜLICH GmbH

KFA

Jül-3258
August 1996
ISSN 0944-2952